

**THE REPUBLIC OF TURKEY  
BAHCESEHIR UNIVERSITY**

**COMPUTER-BASED ATROPHY MEASUREMENT  
ON BRAIN MR IMAGES**

**Master's Thesis**

**GÖKHAN GÖKAY**

**ISTANBUL, 2015**



**THE REPUBLIC OF TURKEY  
BAHCESEHIR UNIVERSITY**

**GRADUATE SCHOOL OF NATURAL AND APPLIED  
SCIENCES  
BIOENGINEERING PROGRAM**

**COMPUTER-BASED ATROPHY  
MEASUREMENT ON BRAIN MR IMAGES**

**Master's Thesis**

**GÖKHAN GÖKAY**

**Thesis Advisor: ASSIST. PROF. DR. DEVRİM ÜNAY**

**ISTANBUL, 2015**

**THE REPUBLIC OF TURKEY  
BAHCESEHIR UNIVERSITY**

**GRADUATE SCHOOL OF NATURAL AND APPLIED SCIENCES  
BIOENGINEERING PROGRAM**

Name of the thesis: Computer-Based Atrophy Measurement on Brain MR Images  
Name/Last Name of the Student: Gökhan GÖKAY  
Date of the Defense of Thesis: 29 May 2015

The thesis has been approved by the Graduate School of Natural and Applied Sciences.

Assoc. Prof. Dr., Nafiz ARICA  
Graduate School Director  
Signature

I certify that this thesis meets all the requirements as a thesis for the degree of Master of Science.

Assoc. Prof. Dr., Gülay BULUT  
Program Coordinator  
Signature

This is to certify that we have read this thesis and we find it fully adequate in scope, quality and content, as a thesis for the degree of Master of Science.

Examining Comittee Members

Signature

Thesis Supervisor  
Assist. Prof. Dr., Devrim ÜNAY

Member  
Prof. Dr., Çiğdem EROĞLU ERDEM

Member  
Assoc. Prof. Dr., Mustafa KAMAŞAK

## ACKNOWLEDGEMENTS

First and foremost I would like to thank my advisor Assist. Prof. Devrim Ünay for his invaluable guidance, support throughout my study and shape my engineering future. I very much appreciate for his suggestions, detailed reviews, invaluable advices, and life lessons. I feel privileged to be his student.

I would like to thank to all members of the BAU-MIP including İlkay Öksüz, Leonardo Itheme, Tuğberk Kocatekin, Oguz Demir and Volkan Özdemir for their constant suggestions for improvement.

I am sincerely grateful to my thesis committee members, Prof. Dr., Çiğdem Eroğlu Erdem and Assoc. Prof. Dr., Mustafa Kamaşak for their invaluable feedback.

I would like to thank to Bayındır Hospital and their valuable experts; Dr., Melek Kandemir, Dr. M.Savaş Tepe, and Dr., Betül Yalçın for helping to create the database.

I would also like to express my deepest gratitude for my beloved family, who always believed in me and always tried their best to make things easier for me.

Finally I would like to acknowledge Bahçeşehir University for supporting me throughout my graduate education.

İstanbul, 2015

Gökhan GÖKAY

## ABSTRACT

### COMPUTER-BASED ATROPHY MEASUREMENT ON BRAIN MR IMAGES

Gökhan GÖKAY

Bioengineering Program

Thesis Supervisor: Assist. Prof. Dr. Devrim Ünay

May 2015, 56 Pages

Diagnosis and treatment of various brain disorders occurring due to aging, has an important place in contemporary research as elderly population in the world and in our country is progressively increasing. Dementia, defined as progressive loss in cognitive skills such as learning, memory, orientation, and language, is a devastating and irreversible brain syndrome mainly affecting the elderly. Cerebral atrophy, defined as neuronal loss or cell death affecting part or all of the brain, is a feature observed in dementia. To determine the presence and severity of atrophy, experts visually evaluate magnetic resonance (MR) images of the brain, especially at locations such as lateral ventricles (LV) and central sulci (CS).

The aim of this thesis study is to manually and automatically measure the sizes of lateral ventricles and central sulci and to compare these measurements with experts' atrophy ratings. Accordingly, in this thesis work we present computer-based, automated solution to quantify geometric features (e.g. length, width, area and volume) and to capture atrophy in LV and CS, and compare these results with visual atrophy ratings provided by experts on subjects with complaints of memory or cognitive ability. The dataset consists of brain MRIs (at varying resolutions and slice thickness values) of 20 subjects taken from routine clinical practice and are visually graded for atrophy by neurology and radiology experts.

The presented study is important for two reasons: (1) it provides an automated solution for measuring atrophy rate from MR data, and (2) therewith it may contribute to the understanding of dementia diagnosis.

**Key Words:** Brain Atrophy, Expert Grading, Lateral Ventricle, Central Sulcus, Automatic Size Measurement

## ÖZET

### BEYİN MR GÖRÜNTÜLERİ ÜZERİNDE BİLGİSAYAR TEMELLİ ATROFİ ÖLÇÜMÜ

Gökhan GÖKAY

Biyomühendislik Programı

Tez Danışmanı: Yrd. Doç. Dr. Devrim Ünay

Mayıs 2015, 56 Sayfa

İnsan beyninde yaşlanmaya bağlı olarak meydana gelen çeşitli hastalıkların teşhisi ve tedavisi, dünyada ve ülkemizde yaşlı nüfusun doğrusal olarak artmasına paralel olarak, günümüz araştırma konularında önemli bir yer tutmaktadır. Demans genelde yaşlanmaya bağlı olarak ortaya çıkan unutkanlığın ön planda olduğu Alzheimer gibi birçok hastalığı içerisinde bulunduran genel semptomlar dizisidir ve 65 yaş üstü grupta sık rastlanan durumların başında gelmektedir. Hücre ölümüne bağlı doku kaybı olarak tanımlanan serebral atrofi, beynin bir kısmını ya da tümünü etkileyen ve demans vakalarında görülebilen bir özelliktir. Atrofi varlığının ve siddetinin belirlenmesi amacıyla uzmanlar manyetik rezonans (MR) görüntülerini kullanarak lateral ventrikül ve sulkuslar gibi beyin bölgelerinin görsel değerlendirmelerine başvurmuşlardır.

Bu tez çalışmasının amacı, demansla ilişkili olduğu düşünülen lateral ventrikül ve santral sulkus boyutlarının hem elle hem de otomatik olarak ölçülmesi ve bu ölçümlerin uzmanların atrofi derecelendirmeleriyle uyumunun incelenmesidir. Bu bağlamda, unutkanlık şüphesi ile hastaneye başvurmuş vakaların MR görüntülerinden lateral ventrikül ve santral sulkus yapılarının uzunluk, genişlik, alan ve hacim gibi değerleri ölçen ve bunları uzman atrofi derecelendirmeleri ile kıyaslayan görüntü işleme temelli bir çalışma sunulmuştur. Ölçüm sonuçlarının kıyaslanması için rutin klinik ortamdan alınan 20 vakanın farklı çözünürlük ve kesit kalınlıklarına sahip MR verisi nöroloji ve radyoloji uzmanlarından oluşan bir ekip tarafından görsel olarak değerlendirilmiş ve atrofi derecelendirmesi yapılmıştır.

Sunulan çalışma, atrofi miktarının MR görüntülerinden otomatik belirlenmesi ve bu probleme yönelik bilgi birikiminin oluşturulması anlamında önem taşımaktadır.

**Anahtar Kelimeler:** Beyin Atrofisi, Uzman Derecelendirmesi, Lateral Ventrikül, Santral Sulkus, Otomatik Boyut Ölçümü

## CONTENTS

TABLES.....	x
FIGURES.....	xi
ABBREVIATIONS .....	xiii
1.INTRODUCTION .....	1
1.1 RESEARCH OVERVIEW .....	1
1.2. CONTRIBUTIONS OF THE THESIS.....	4
1.3 THESIS OUTLINE .....	5
2.LITERATURE REVIEW .....	6
3.METHODS .....	9
3.1 PATIENT DATABASE AND GRADING .....	9
3.1.1 Sulcal Atrophy Grading .....	10
3.1.2 Ventricular Atrophy Grading.....	10
3.2 SEGMENTATION .....	10
3.2.1 Segmentation of Lateral Ventricles.....	11
3.2.2 Segmentation of Central Sulci .....	12
3.3 SKELETONIZATION .....	14
3.3.1 Separating Segmentation Results.....	14
3.3.2 Preprocessing for Skeletonization.....	16
3.3.2 Skeletonization in 2D Images .....	17
3.3.3 Skeletonization in 3D.....	21
3.4 MEASUREMENT AND ATROPHY QUANTIFICATION .....	24
4.RESULTS .....	26
4.1 MEASUREMENT AND CORRELATION RESULTS .....	26
4.1.1 2D Measurement Results of LV.....	26



4.1.2 2D Measurement Results of CS .....	29
4.1.3 3D Measurement Results of LV .....	31
4.1.4: 3D Measurement Results of CS .....	33
5.DISCUSSIONS AND RESULTS .....	35
5.1 RESULTS .....	36
5.2 FUTURE WORKS .....	37
REFERENCES.....	38
CURRICULUM VITAE.....	43

## TABLES

Table 4.1: 2D LV Measurement Results.....	27
Table 4.2: 2D CS Measurement Results .....	29
Table:4.3 3D LV Measurement Results.....	31
Table 4.4: 3D CS Measurement Results .....	33
Table 4.5: Correlation Results of the Database.....	35

## FIGURES

Figure 1.1: Lateral Ventricles in Brain Drawing .....	2
Figure 1.2: Lateral Ventricles in T1 MRI .....	2
Figure 1.3: Central Sulcus in Brain Drawing.....	3
Figure 1.4: Central Sulci in T1 MRI.....	3
Figure 1.5: Project main flowchart.....	4
Figure 3.1: Atrophy Scale .....	10
Figure 3.2: LV automatically segmented on Axial T1-weighted MRI and displayed in 2D.....	11
Figure 3.3: Automated segmentation result of LV reconstructed in 3D .....	12
Figure 3.4: CS manually segmented on Axial T1-weighted MRI and displayed in 2D .	13
Figure 3.5: Manual segmentation result of CS reconstructed in 3D .....	13
Figure 3.6: Detection of inter-hemispheric fissure .....	14
Figure 3.7: Applying RANSAC algorithm to fit a line to an arbitrary noisy data.....	15
Figure 3.9: Examples of problematic LV segmentations obtained by ALVIN.....	17
Figure 3.10: 2D Skeletonization Process Flowchart .....	18
Figure 3.11: 2D Skeletonization of Right CS .....	19
Figure 3.12: Geodesic distance based detection of CS medial axis. The detected path is highlighted in red for visual purposes.....	20
Figure 3.13: Geodesic distance based detection of LV medial axis. The detected path is highlighted in red for visual purposes.....	20
Figure 3.14: 3D Skeletonization Process Flowchart .....	21
Figure 3.15: Exemplary 3D skeletonization for right LV .....	22
Figure 3.16: 3D Skeleton path on Right CS.....	23

Figure 3.17: Size change in lateral ventricles in comparison to atrophy degree.....	24
Figure 3.18: 2D Skeletonization Process on LV .....	25
Figure 3.19: 2D Skeletonization Process on CS .....	25
Figure 4.1: Scatter plots of 2D LV measurements versus expert grades .....	28
Figure 4.2: Scatter plots of 2D CS measurements versus expert grades.....	30
Figure 4.3: Scatter plots of 3D LV measurements versus expert grades .....	32
Figure 4.4: Scatter plots of 3D CS measurements versus expert grades.....	34

## ABBREVIATIONS

2D	:	2 Dimensional
3D	:	3 Dimensional
MRI	:	Magnetic Resonance Imaging
LV	:	Lateral Ventricle
CS	:	Central Sulcus
CSF	:	Cerebrospinal Fluid
PC	:	Posterior Commissure
AC	:	Anterior Commissure
WM	:	White Matter
Voxel	:	Volumetric Pixel
CSF	:	Cerebrospinal Fluid
ID	:	Identification

## **1. INTRODUCTION**

Introduction of the thesis starts with description of the dementia in the overview part, after that, contributions of the thesis is explained and then we give outline of the thesis.

### **1.1 RESEARCH OVERVIEW**

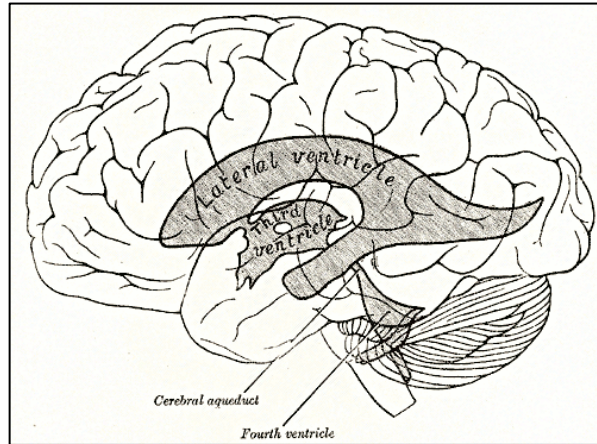
Dementia can be described as progressive loss with cognitive functions such as memory, language, and reasoning, planning, recognizing, or identifying people or objects. Also dementia is a devastating and irreversible brain syndrome. This decline is beyond what might be expected from normal aging. Dementia can have bad affects on daily activities such as cooking, walking, driving, and even personal care activities such as bathing, dressing, and feeding. The probability of dementia increases with age. Dementia generally is shown in the second half of life, often after the age of 65. (van de Pol et al., 2009, Scheltens et al., 1992 ). Dementia usually progresses slowly. Making an accurate diagnosis in the early stages of dementia is very difficult and also important. It is important to confirm a diagnosis of dementia to find out itself and degree of dementia.

Diagnosis dementia is generally done with combined analysis of different cases such as cognitive skills, demographic status, family history, and neuroimaging results, in example: degree and distribution of atrophy can help to diagnose dementia which can be measured from neuroimaging results. Measurement based on these findings from images is generally performed by experts' visual assessment. And also there are some researches for rating dementia based on neuroimaging findings with cerebral atrophy degree and white matter (WM) lesions (Yue et al., 1997, Nestor et al., 2008).

In this project we are going to use LV and CS measurement based length, width, area and volume values of each patient to calculate corresponding correlation values. LV can be described as the largest of the ventricles in the human brain. LV is a cavity that filled with cerebrospinal fluid in the human brain and also part of a system of four communicating cavities that are continuous with the central canal of the spinal cord. The lateral ventricles are part of the ventricular system of the brain. There are two lateral ventricles are located in the human cerebral hemispheres, one in each hemisphere. LV has a triangular central body

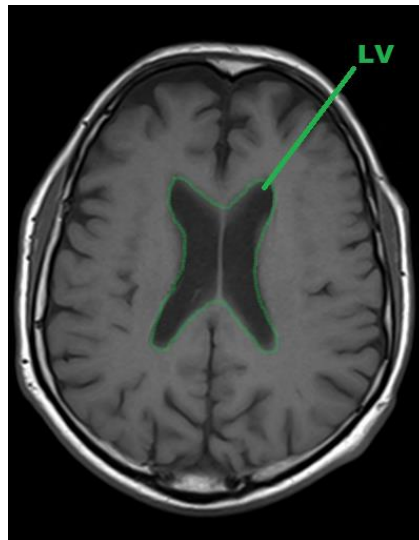
and four horns. The third and fourth ventricles are located in the center of the brain. Both cerebral hemispheres contain a lateral ventricle. The shape of the each lateral ventricle resembles a C-shaped structure that formed by 3 main parts called as a temporal (inferior) horn, posterior (occipital) lobe and frontal (anterior) lobe. Deformation of the shape in LV is related with amount of atrophy. LV can be seen in Figure 1.1 and 1.2.

**Figure 1.1: Lateral Ventricles in Brain Drawing**



Source: Quizlet

**Figure 1.2: Lateral Ventricles in T1 MRI**

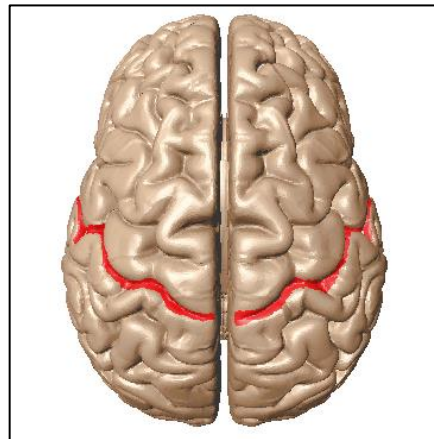


Source: prepared by G.Gökay with Matlab

CS is the biggest one of the 14 sulci in human brain and it separates the frontal lobe, which is controlling emotion and decision mechanisms and the Parietal Lobe, which is

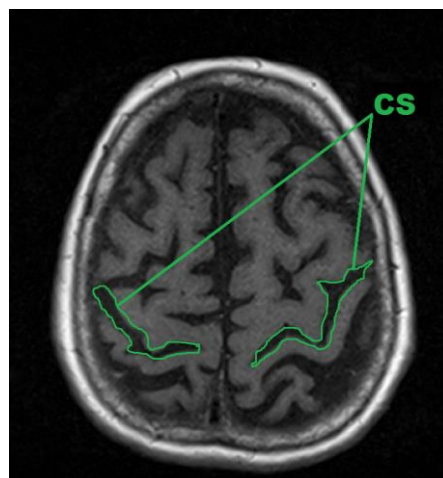
processing sensor signals (e.g. touch, and taste) coming from human body. CS is the only sulcal structure in cerebral cortex that separates the two lobes from each other (Naidich and Brightbill 1996). CS is an important landmark which separates the sensory region from the motor area. It is also important to investigate physical attributes of the CS to diagnose and grade dementia diseases (Barkhof, 2011). From this view, the one leg of the purpose of the project is measuring dementia is related to amount of atrophy in the human brain by using MRI based neuroimaging findings graded with atrophy degree. CS is described in Figure 1.3 and 1.4.

**Figure 1.3: Central Sulcus in Brain Drawing**



Source: Quizlet

**Figure 1.4: Central Sulci in T1 MRI**

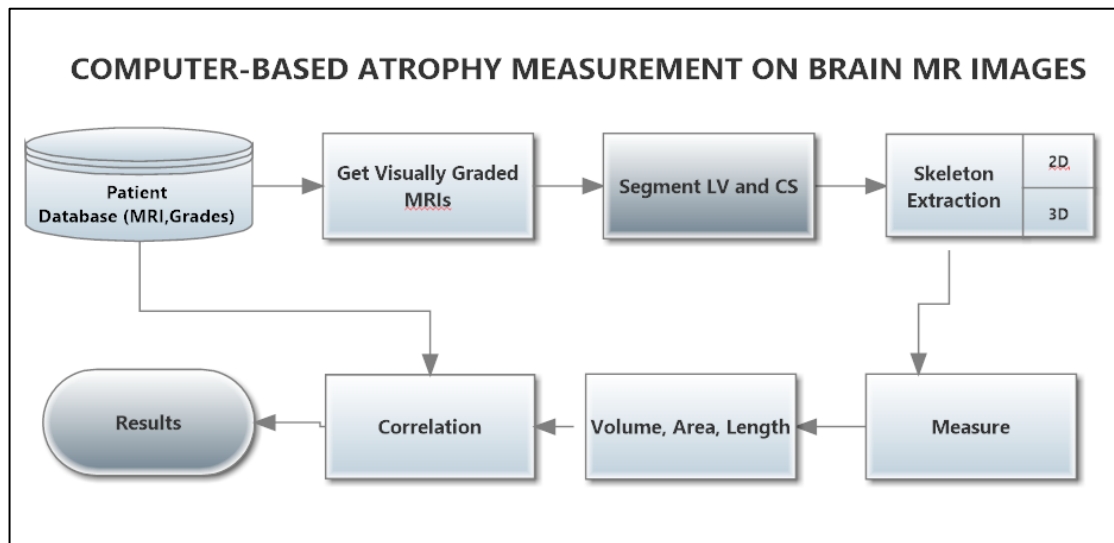


Source: prepared by G.Gökay with Matlab



Accordingly, the purpose of this work is to automatically measure the amount of atrophy in the human brain from MRI and compare these measurements with experts' visual grades. To this end an MR dataset of 20 subjects, collected from routine clinical practice at Bayındır Hastanesi İçerenköy and visually graded with respect to cerebral atrophy by a team of 2 neurologists and 2 radiologists from the same hospital, is used. The project summary can be seen in the following chart in Figure 1.5. In this project we are going to use these MR images in the patient database given in first step of chart, to detect LV's and CS' length, width, area and volume values by doing following steps segmentation, skeleton extraction and measurement to compare the results with atrophy ratings given by experts that subjects with complaints with lost of memory or cognitive ability are admitted to hospital. For the measurements we use computer based approach with manual and automatic way. And then we are going to compare our results with experts' results in the correlation part. Then we obtain the results.

**Figure 1.5: Project main flowchart**



Source: prepared by G.Gökay with Smartdraw

## 1.2. CONTRIBUTIONS OF THE THESIS

In light of the above literature review and the information presented in the Introduction section, there are two main contributions of this thesis study.

1. First of all, a novel neuroimaging dataset consisting of MR images of subjects with complaints of memory or cognitive ability and the corresponding atrophy grades visually assessed by experts is created.
2. Secondly, image processing based novel methods are developed to realize size quantification of LV and CS in both 2D and 3D. Agreement between the resulting measurements obtained over the whole dataset and the corresponding experts' atrophy grades is explored using correlation analysis.

The quantification methods developed and the analyses realized in this thesis study will hopefully provide important insight and information in creating a robust and accurate computer-based atrophy grading system from brain MR images.

### **1.3 THESIS OUTLINE**

The outline of this thesis is as follows.

In Section 2, literature survey and research about atrophy related with central sulcus and lateral ventricles will be summarized.

In Section 3, implementation of the methodology will be discussed in four main parts as grading, segmentation, skeletonization and measurement. In grading section, patient database and grading methodology done by experts will be explained in detail. In the segmentation part we will be giving information about the method we used to segment LV and CS. Skeletonization part is needed for length measurements of LV and CS from 2D and 3D images. For the measurement part we are going to use skeletonization results to obtain the geodesic distance based length measurement for LV and CS.

In Section 4, results of this study will be given with details as numeric values, tables and scatter graphs.

In Section 5, discussions on weaknesses, limitations, and potential future works of the proposed method will be presented.

## 2. LITERATURE REVIEW

Dementia is a health condition affecting the brain with progressive loss in cognitive skills such as learning, memory, orientation, and language. Furthermore, it is a devastating and irreversible brain syndrome badly affecting the social and business lives of its victims (Silverman et al., 1999). The incidence of dementia is increasing in direct proportion with age. It is observed in 10% of people with age 65 years or more, while this rate rises to 50% among people aged 85+. Today, more than 24 million people suffer from dementia in the world. In 2040 people suffer from dementia is expected to exceed 80 million with increased life expectancy (Ferri, et al., 2005). In our country, the number of those in the age group 65+ is about 4 million, according to data of 2000 and in the following years this number is expected to increase even more (Cankurtaran and Arıođul, 2004)

Detection of dementia in the clinical settings depends on combined analysis of data such as patient's cognitive skills, demographic status, family history, and neuroimaging results (such as degree atrophy). Research efforts for the purpose of rating dementia based on neuroimaging related findings have focused on parameters such as cortical/subcortical atrophy and white matter lesions (Scheltens et al., 1992). The dementia syndrome may occur in different forms, where the most common type is Alzheimer's disease causing two-thirds of all cases of dementia (Silverman et al., 1999).

Getting the correct diagnosis and prognosis, due to increasing of the number of people with dementia that we have mentioned previously, is an important priority and status. For treatment of dementia traditional approaches are used to detect curable types of dementia such as neuroimaging can be used to distinguish between different types in recent years. Then, cases for dementia referred to a neurologist practice guidelines offers neuroimaging is proposed to possibly magnetic resonance imaging (MRI), preferences and computed tomography (CT) technique or X-ray imaging techniques (Waldemar et al., 2000).

In addition, shrinkage of the brain known as cerebral atrophy emerges as a promising research topic for the diagnosis of dementia in recent years. As an example researchers

explore the relationship between cerebral atrophy and cognitive and behavioral functions (Miller, 2002). In clinical practice, diagnosis of dementia depends usually on cognitive skills, patient's demographic situation, dementia in the family history, and neuroimaging results (van de Pol, et al., 2009, Scheltens et al., 1992).

In general cerebral atrophy, frequently observed in dementia patients, is defined as deterioration of brain neurons and loss of their interconnections. So in this study we are going to implement an automatic, computer based approach to measure the amount of atrophy in the human brain, specifically in lateral ventricles and central sulci. The atrophy grading of these findings from images are done by experts' visual assessments while we used computer-based approach to compare the results.

Studies with computer-based measurement of atrophy findings are limited, and generally focus on evaluation of medial temporal lobe atrophy. There are also studies which uses computer based approach to measure atrophy specifically in the selected areas ( i.e.: grey matter, basal ganglia, hippocampus and adjacent cortex ) of the brain (Tosun et al., 2007, Giesel, et al., 2006, Rettmann et al., 2006). Studies using computer-based measurement are mostly focused on the measurement of only one parameter associated with dementia and the methodology cannot be expanded to other structures in the brain. For example cortical and subcortical atrophy (Raya et al., 1990) or medial temporal lobe atrophy (Giesel, et al., 2006).

To measure atrophy with computer-based approaches, semi-automatic (Whitwell et al., 2007, Bell-McGinty et al.,2005 ) and automatic (Tosun et al.,2009, Tosun et al.,2007) methods have been proposed recently. In the work of MacKenzie et al., (2002) patients with traumatic brain injury undergo longitudinal MRI scanning, from which brain and cerebrospinal fluid regions are found by semi-automatic segmentation based on fuzzy logic. And the amount of decrease in the brain parenchyma volume is measured. Whitwell et al., (2007) and Bell-McGinty et al., (2005) employed a semi-automated method based on voxel-based morphometry, and calculated the gray matter reduction in the images taken from the same patient at different times. In Rettmann et al., (2006) eight different sulci from the MR data of healthy individuals are found by manually marking and watershed-based segmentation to measure atrophy in these regions; brain surface area, gray matter thickness / volume, sulcus depth, local gyrification index and

curvature were used as atrophy measures. In Scher et al., (2007), temporal MR data is processed semi-automatically to detect decrease in intracranial volume.

The automatic method proposed in Rettmann et al., (2006) utilized the CRUISE software tool, which achieves implicit surface evolution of the cortex, to measure gray matter thickness, depth of the sulcus and curvature, and is evaluated on Parkinson (Tosun et al.,2007) and Alzheimer (Tosun et al.,2009) datasets.

Above literature review demonstrates that prior art exists on cerebral atrophy quantification from MRI data. Assessment of dementia related neuro-imaging findings such as cortical / subcortical atrophy is generally done by experts manually or using semi-automated or automated solutions. Nevertheless, to the best of our knowledge there is prior work on automated measurement of atrophy in lateral ventricles and central sulci, and comparison of these measurements with experts' visual ratings from MRI. Such a computer-based automated measurement system will provide quantitative, robust, and consistent measurements, which may provide the experts with important insight regarding the disease and assist them towards better diagnosis and prognosis.

Accordingly, the solution developed in this thesis study works for both 2D and 3D real MRI images with different slice thicknesses, and is evaluated with a database collected at the Department of Radiology Bayındır Hastanesi İçerenköy and visually graded for atrophy by experts therein.

### 3. METHODS

In this section of the thesis we will detail the methods we used to realize computer based measurement of LV and CS structures from MR data. More specifically, we will respectively explain the patient database and the grading employed, segmentation of the structure, skeletonization of the segment found, and the measurement and quantification realized.

#### 3.1 PATIENT DATABASE AND GRADING

In the medical field, access to imaging data is difficult due to patient privacy and security of medical information as well as disease-specific data collection. Nevertheless, in this work we use brain MR data of 20 elderly subjects collected at routine clinical practice and visually assessed for sulcal atrophy and ventricular enlargement by field experts. The aforementioned subjects are admitted to the hospital due to complaints regarding progressive loss in cognitive skills such as learning, memory, orientation, and language.

Neuroimaging of the subjects is realized at the Department of Radiology of Bayındır Hospital İçerenköy using a 1.5T scanner (Siemens, Germany). Details of the imaging protocol used are as follows:

T1 turbo spin echo axial TR/TE 367/12, slice thickness 3.6 mm, number of cross-sections 40, “intersection gap” 0.6 mm, matrix 512x424, “averages” 1, “field of view” 236 mm. T1-weighted spin echo axial images with 3.6mm and 6.0 mm slice thickness are used in this study.

Additionally, a team of two neurologists and two radiologists from Bayındır Hospital İçerenköy performed visual assessment of cerebral atrophy on each subject data in a similar fashion to the procedure of Yue, et al (1997). In a nutshell, each subject’s MR data is visually evaluated and graded (in consensus agreement) on a semi-quantitative 10-point scale using a separate reference data. The scale can be seen in Figure 3.1.

### 3.1.1 Sulcal Atrophy Grading

For sulcal atrophy, the axial slice best exposing the central sulci is selected and visually assessed on a semi-quantitative 10-point scale where 0 indicates no atrophy and small sulci, while 9 indicates high atrophy and very large sulci.

### 3.1.2 Ventricular Atrophy Grading

Visual assessment of ventricular enlargement is realized in a similar fashion to sulcal atrophy grading. The axial slice best exposing the lateral ventricles (LV) is selected and the subject data is visually assigned one of 10 grades in accordance with the reference data set (0 indicates absence of atrophy and small LV, while 9 indicates high atrophy and highly enlarged LV).

**Figure 3.1: Atrophy Scale**

<b>Ventricular / Sulcal Atrophy</b>	
<b>Degree</b>	<b>Grade</b>
<b>Low</b>	<b>0</b>
	<b>1</b>
	<b>2</b>
	<b>3</b>
	<b>4</b>
	<b>5</b>
	<b>6</b>
	<b>7</b>
<b>High</b>	<b>8</b>
	<b>9</b>

Source: prepared by G.Gökay with Microsoft Word

## 3.2 SEGMENTATION

Rapid advances in the field of medical imaging facilitate the medicine by the value of engineering. The determination of disease is the first step of clinical care for a patient. The use of computer-aided diagnosis (CAD) systems is used for diagnosis to provide more confidence in their decisions. A computer-aided diagnosis system generally needs a specific part of the medical imaging related with the disease. And these statements

introduce us with concept named segmentation. Below we are going to explain how LV and CS are segmented both manually and automatically in this study.

### 3.2.1 Segmentation of Lateral Ventricles

Comparing visual assessment grades with manual and automatic measurement results starts with preprocessing T1 MRI images to segment LV in our database for measuring ventricular enlargement to segment LV on the database. In order to automatically segment LV in 3D, we use freely available Automatic Lateral Ventricle delineation (ALVIN) v1.05 tool (<https://sites.google.com/site/mrilateralventricle/>) (Kempton, et al, 2011) that runs on Matlab with SPM8 (<http://www.fil.ion.ucl.ac.uk/spm/>). ALVIN assumes that LV's are the largest empty regions close to the center of weight of the brain in T1-weighted images. ALVIN uses a binary mask to spatially normalized cerebral spinal fluid (CSF) segmented images produced using unified segmentation. (Kempton, et al, 2011) In addition, experts manually delineate LV on cross-sectional images of each subject data. This binary mask is then used to validate accuracy of automated segmentations realized by ALVIN. Figures 3.2 and 3.3 display automatic LV segmentation results in 2D and 3D, respectively.

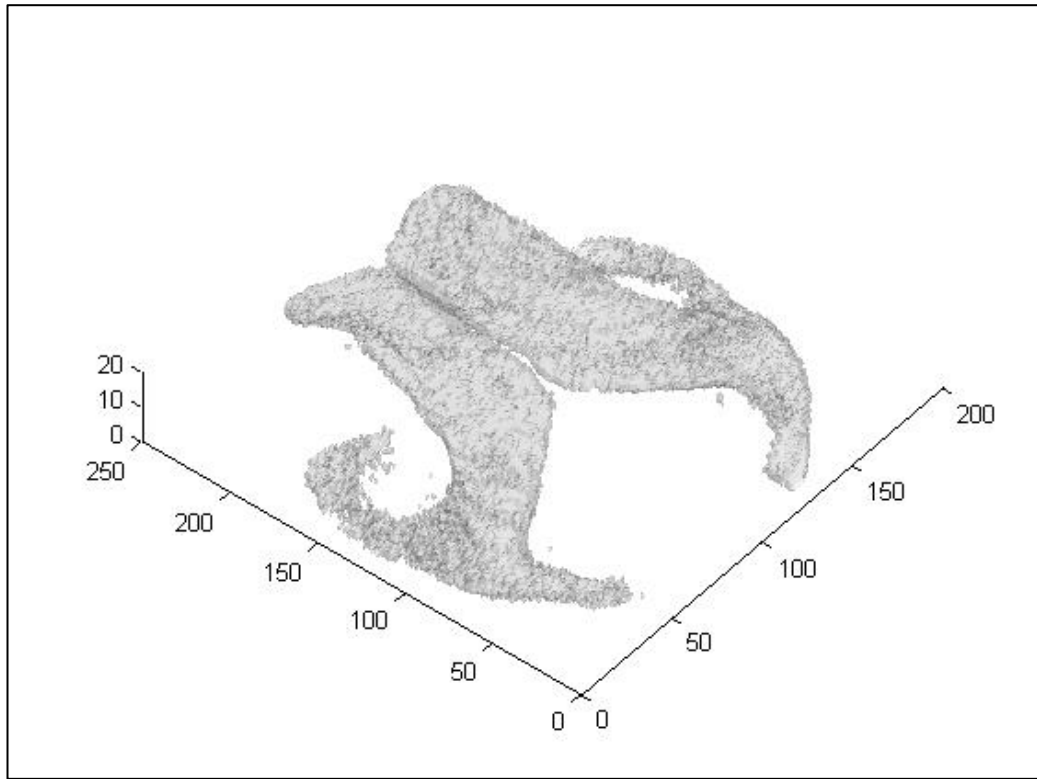
**Figure 3.2: LV automatically segmented on Axial T1-weighted MRI and displayed in 2D**



Source: prepared by G.Gökay with Matlab



**Figure 3.3: Automated segmentation result of LV reconstructed in 3D**



Source: prepared by G.Gökay with Matlab

### **3.2.2 Segmentation of Central Sulci**

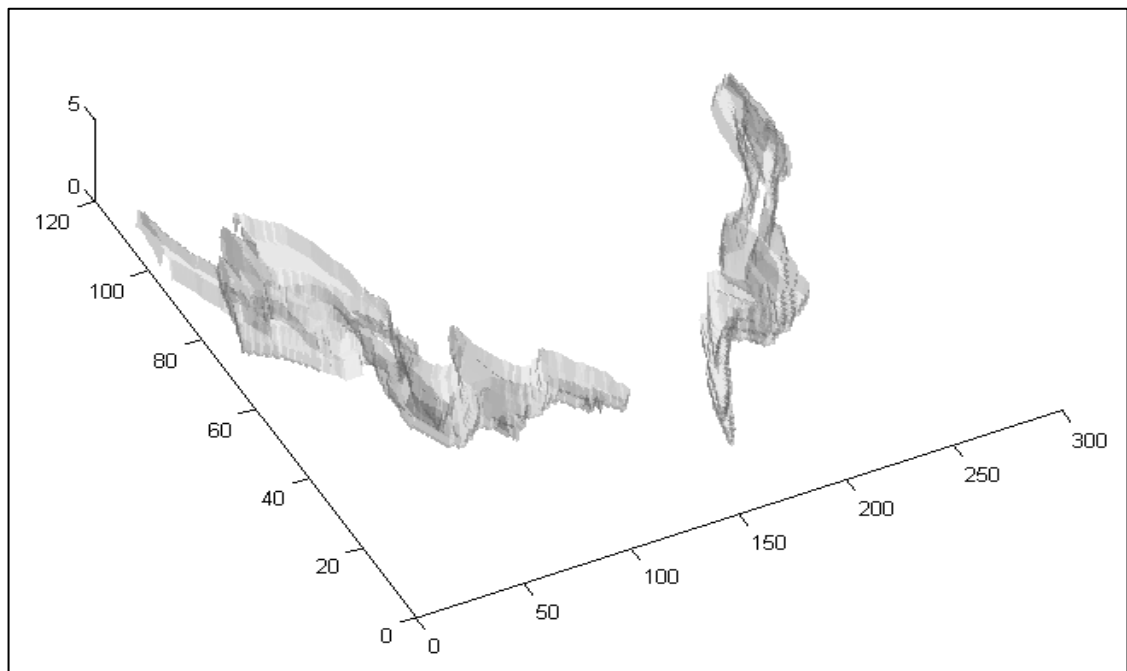
For atrophy quantification in central sulci we need automated segmentation of these structures. However, to the best of our knowledge there is no robust segmentation algorithm proposed to automatically segment CS in the literature. For this purpose we use the automatic CS segmentation algorithm developed by O. Demir (2013) in his Master's thesis study under the supervision of Dr. Ünay. The algorithm finds candidate CS locations via an atlas-based approach, and finalizes segmentation using region growing. Likewise in LV, experts' manual delineations of CS are obtained as well for comparative evaluation. Figures 3.4 and 3.5 show manual segmentations of CS in 2D and 3D, respectively.

**Figure 3.4: CS manually segmented on Axial T1-weighted MRI and displayed in 2D**



Source: prepared by G.Gökay with Matlab

**Figure 3.5: Manual segmentation result of CS reconstructed in 3D**



Source: prepared by G.Gökay with Matlab

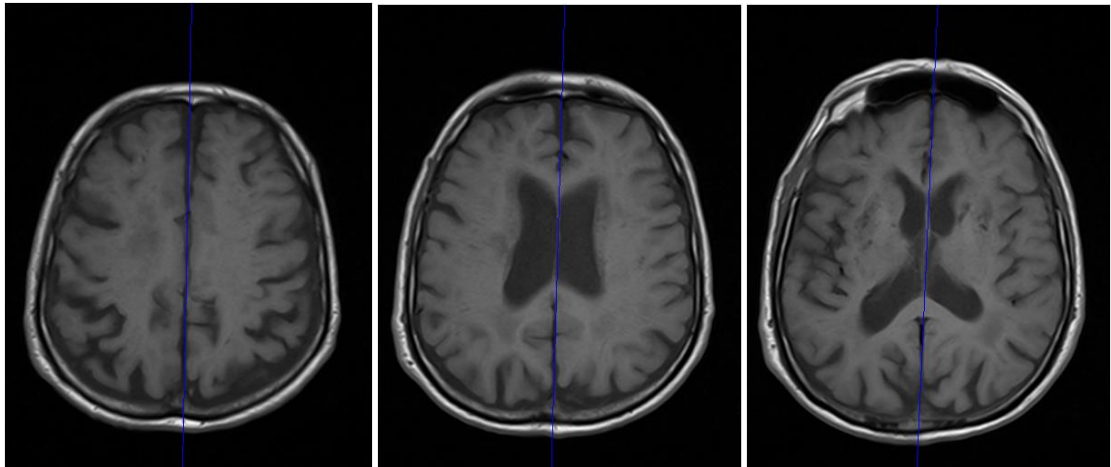
### 3.3 SKELETONIZATION

Skeletonization is a process to extract medial axis of a binary object in 2D or 3D. In general segmentation of the brain tissues' or structures have arbitrary shapes. So measuring length information is not easy to calculate. To this end, we use obtained skeleton to correctly and effectively measure length of arbitrary shapes. We have implemented two different skeletonization algorithms to handle 2D and 3D skeletonization of LV and CS.

#### 3.3.1 Separating Segmentation Results

As mentioned before LV and CS are symmetrically distributed along the hemispheres in the human brain. Thus, hemispheric parts of these two structures must be separated first. This process is not difficult for CS as its parts are well separated and distant from each other. However, LV is a connected structure extending to each hemisphere. Therefore in this work its separation is realized using the inter-hemispheric fissure, which is the border line between the two cerebral hemispheres (Figure 3.6).

**Figure 3.6: Detection of inter-hemispheric fissure**



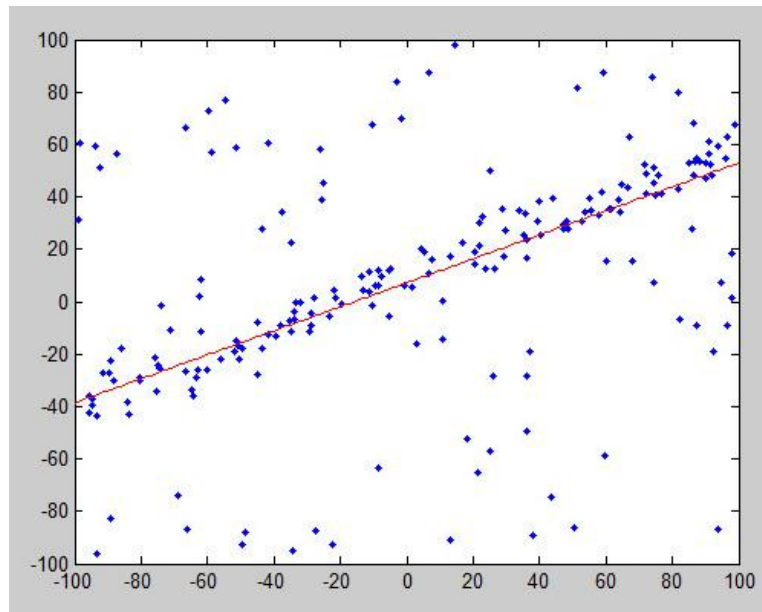
Source: prepared by G.Gökay with Matlab

We use a RANSAC (Random sample consensus) based algorithm presented by Ekin (2005) to detect inter-hemispheric fissure line in brain MR images (Figure 3.6). The algorithm works as follows;

1. Randomly select a subset of the data set
2. Fit a model to the selected subset
3. Determine the number of outliers
4. Repeat steps 1-3 for a prescribed number of iterations

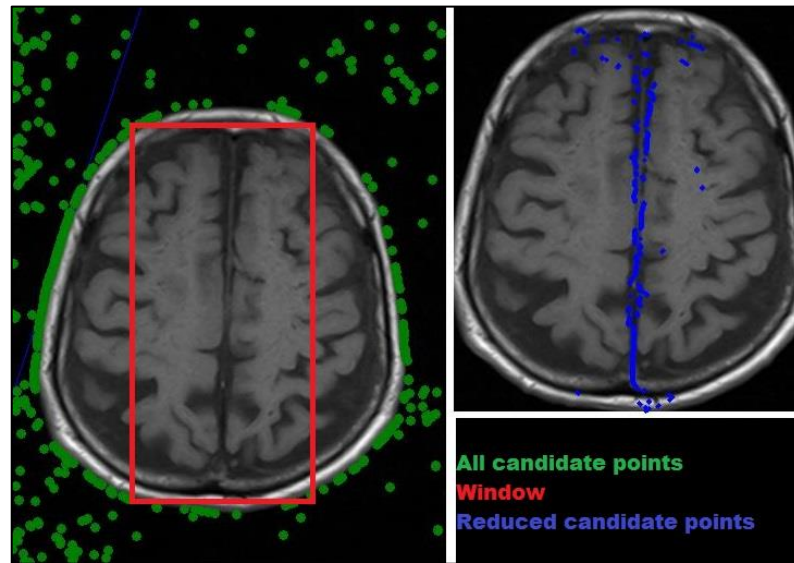
In general applying RANSAC for a data subset showed in the Figure 3.7. To apply this algorithm we randomly generate candidate points from dark regions of axial T1-weighted MRIs. Then we push a window has seen in the Figure 3.8 in red to constrict candidate points. And then we get inter-hemispheric fissure line. After getting the line we use to spate both LV and CS for Left and Right parts.

**Figure 3.7: Applying RANSAC algorithm to fit a line to an arbitrary noisy data**



Source: Mathworks

**Figure 3.8: Applying RANSAC algorithm in MRI data**

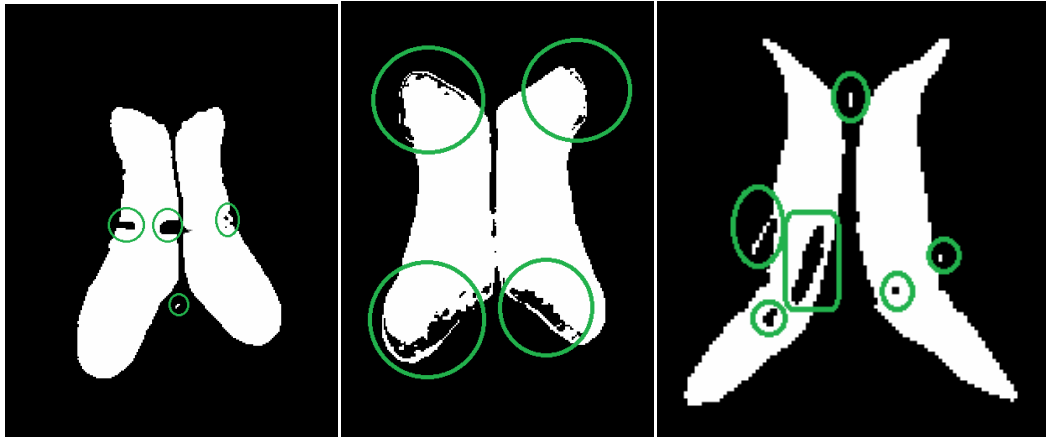


Source: prepared by G.Gökay with Matlab

### **3.3.2 Preprocessing for Skeletonization**

ALVIN segmentation results may sometimes have isolated and unnecessary parts or missing holes in LV (Figure 3.9). To obtain the best fitting skeleton we need to handle these areas with basic preprocessing techniques without deforming the LV structure. For this purpose, first we remove isolated and small (pixel area smaller than 50) segments by using connected component analysis. Then we apply a sequence of binary morphologic operations (namely 'majority', 'open', and 'fill' from the Image Processing Toolbox of Matlab) to get rid of the holes.

**Figure 3.9: Examples of problematic LV segmentations obtained by ALVIN**

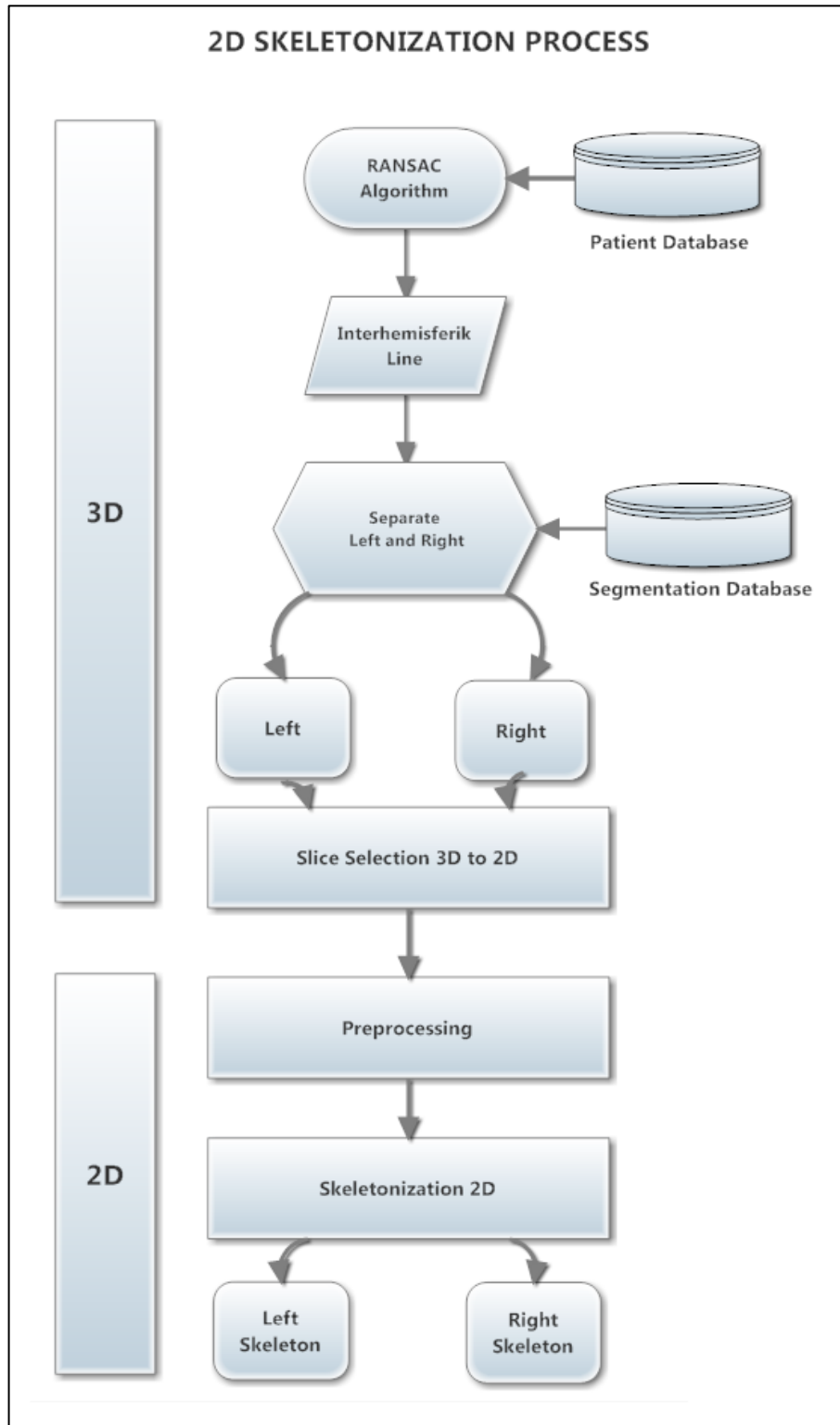


Source: prepared by G.Gökay with Matlab

### **3.3.2 Skeletonization in 2D Images**

As summarized in Figure 3.10, 2D skeletonization starts with separating LV and CS into their hemispherical counterparts. After that we need to select the slice on which we are going to initiate skeletonization. As mentioned in the literature review, widths of LV and CS are directly related to the amount of atrophy in the human brain, so we decided to select the slice where largest cross-sectional area of the structure-of-interest is visible. After selecting the ‘best’ slice, we apply preprocessing to get better skeletonization results.

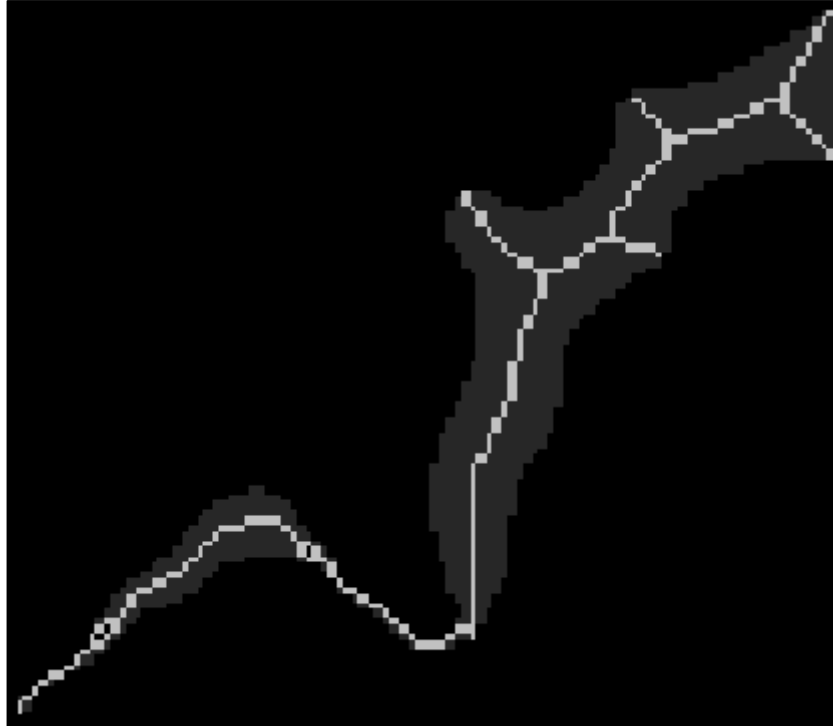
Figure 3.10: 2D Skeletonization Process Flowchart



Source: prepared by G.Gökay with Smartdarw

In this work, 2D skeletonization is realized by using Matlab's built-in binary skeleton algorithm, which iteratively removes pixels on the outer boundaries of objects while not allowing objects to break apart. Resulting skeleton is a single pixel wide medial axis of the object-of-interest (Haralick and Shapiro, 1992). As seen in Figure 3.11 binary skeleton algorithm works properly for right CS.

**Figure 3.11: 2D Skeletonization of Right CS**



Source: prepared by G.Gökay with Matlab

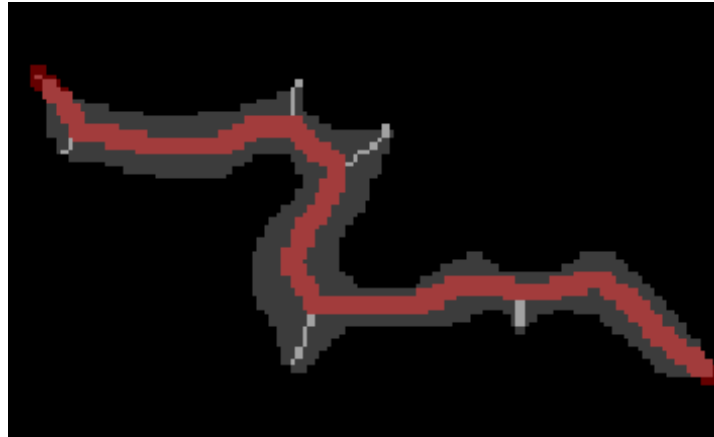
Next we need to find the length of the skeleton fitting the structure. Due to the complicated geometry of LV and CS (e.g. LV appear curved in 2D and horseshoe-shaped in 3D), a straightforward distance measurement such as L2-norm between the end points of their skeletons will be inaccurate. Hence we used geodesic distance (Soille, 2003), which measures the shortest skeleton path between its end points.

Accurately locating the actual end points of the skeleton is a challenge due to the presence of protrusions on the skeleton. To overcome this challenge, we first locate all candidate end points, and calculate geodesic distances between all possible end points pairs. The pair with the largest distance is assumed to belong to the actual end points and the corresponding distance is assigned as the length of the skeleton. Exemplary



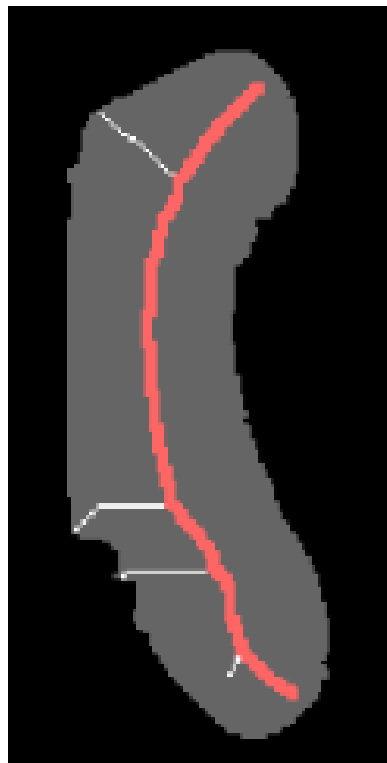
results of this approach are shown in Figures 3.12 for LV and 3.13 for CS where end points are accurately located and the correct medial axis is highlighted

**Figure 3.12: Geodesic distance based detection of CS medial axis. The detected path is highlighted in red for visual purposes.**



Source: prepared by G.Gökay with Matlab

**Figure 3.13: Geodesic distance based detection of LV medial axis. The detected path is highlighted in red for visual purposes.**

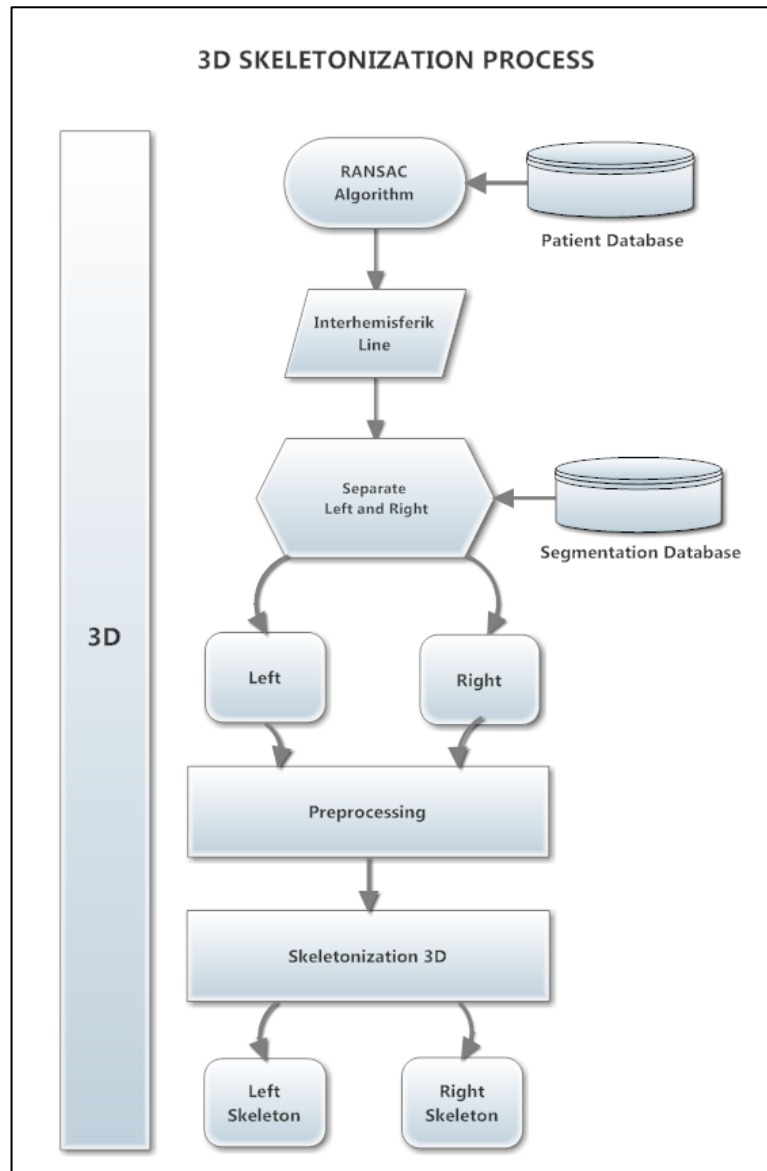


Source: prepared by G.Gökay with Matlab

### 3.3.3 Skeletonization in 3D

Similar to the 2D skeletonization approach explained above, extraction of 3D skeleton starts with separating the LV and CS segmentations into left and right parts. After that, we use the fast marching based skeletonization algorithm (Hassouna et. all, 2007 and Uitert et. all, 2007). Flowchart of the 3D skeleton extraction approach we propose is displayed in Figure 3.13.

**Figure 3.14: 3D Skeletonization Process Flowchart**

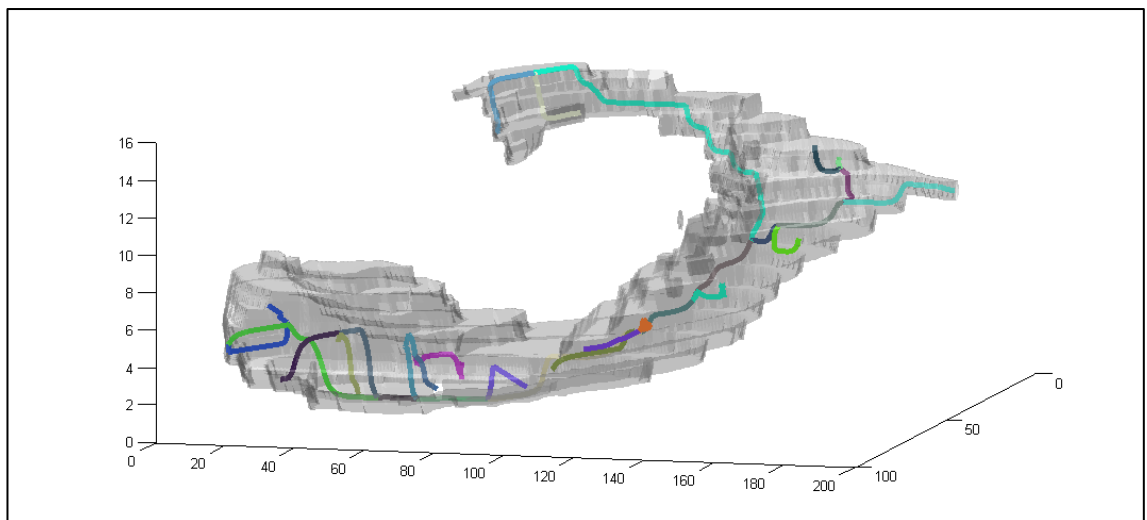


Source: prepared by G.Gökay with Smartdraw

3D skeletonization method uses fast marching algorithm to generate distance transform introduced by Sethian (1996). For 3D segmentation results of LV and CS, we used Dirk-Jan Kroon's implementation (<http://www.mathworks.com/matlabcentral/fileexchange/24531-accurate-fast-marching>) done in Matlab using C language to accelerate calculation. The theory behind the algorithm is Uiter's work (2007) and done by Matlab binary skeleton algorithm.

The algorithmic solution that we use to extract skeleton in 3D generates lines with branches in the inner boundaries of the image. The sum of all colored skeleton lines constraints the skeleton of 3D image in the Figure 3.15. As seen in the right LV example displayed in Figure 3.15, 3D skeletonization algorithm outputs acceptable results.

**Figure 3.15: Exemplary 3D skeletonization for right LV**

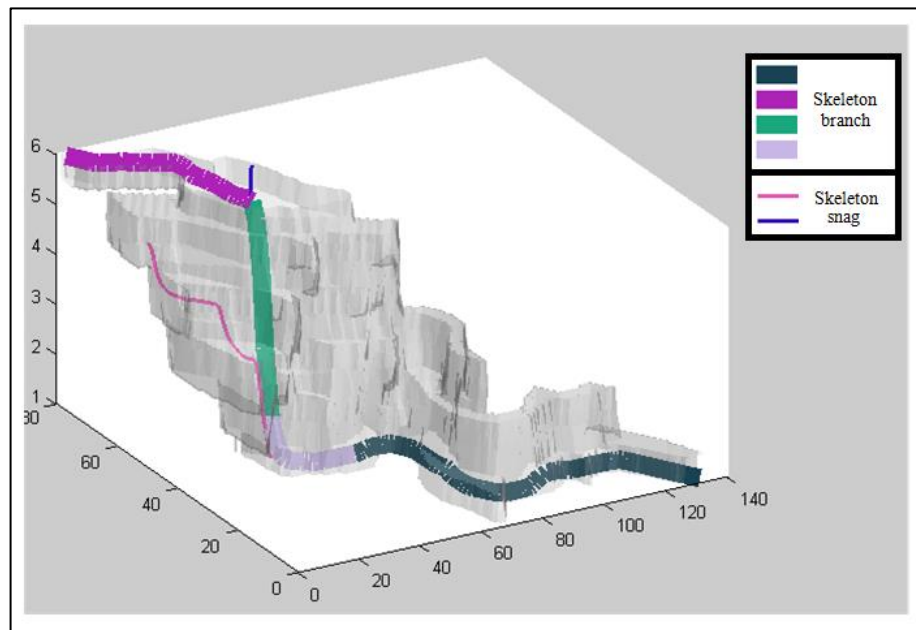


Source: prepared by G.Gökay with Matlab

The output of the 3D skeletonization algorithm consists of the actual medial axis as well as additional protrusions due to the complicated shape of the structure-of-interest (Figure 3.15). In order to quantify the level of atrophy in a structure we need to detect the actual medial axis and compute its length. To this end, like in the 2D case, we locate candidate end points of the skeleton, compute geodesic distance based shortest path between every possible end point pair, and take the pair with the longest distance. All these steps are realized in 3D this time and the final end point pair is set as the start and end points of the actual skeleton, and the corresponding distance value is assigned as the

structure's length. Figure 3.16 displays an exemplary result where the actual skeleton is highlighted.

**Figure 3.16: 3D Skeleton path on Right CS**

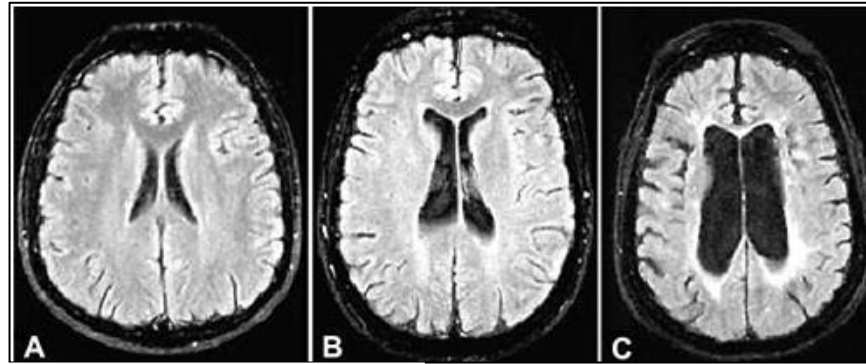


Source: prepared by G.Gökay with Matlab

### 3.4 MEASUREMENT AND ATROPHY QUANTIFICATION

Size of lateral ventricles is considered to be a biomarker for cerebral atrophy (Portaccio et al. 2012). An exemplary image from the literature nicely outlines this relationship where dilation in lateral ventricles is accompanied with higher levels of atrophy (Figure 3.16).

**Figure 3.17: Size change in lateral ventricles in comparison to atrophy degree**



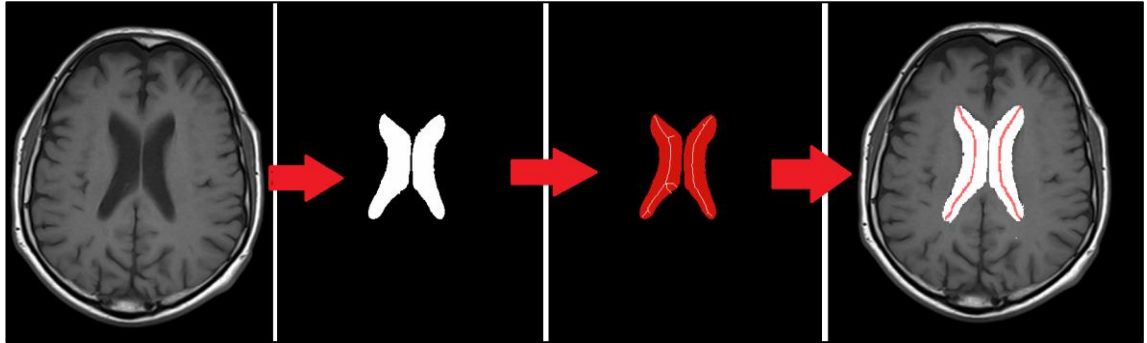
Source: Portaccio et al. 2012

In this section we are going to explain how we will use the extracted skeletons (detailed in the previous section) to obtain length, width, cross-sectional area, and volume measurements for CS and LV. And then we are going to correlation scores between these measurements and experts' grades.

As 2D measurements we focus on area, length, and width of LV and CS. To measure the length we use the geodesic distance based approach calculated on the skeleton and explained previously. Binary segmentation results are used to compute the area measure for each structure. The (average) widths of the structures are then approximated as the ratio between the area and the length measures. These measurements are repeated for both automatic and manual segmentations.

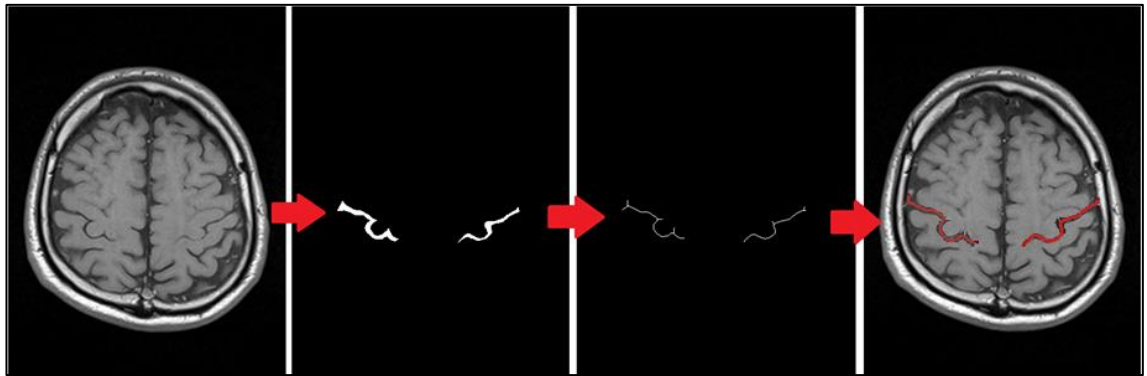
Furthermore, these measurements are manually realized by an expert on the same MR slice, where for each subject data the expert delineated the boundary of the structure (area), its medial axis (length) and its width at multiple equispaced locations perpendicular to and along the medial axis (average width). All system for skeletonization in 2D work can be summarized as in figure 3.16 for LV and 3.17 for CS.

**Figure 3.18: 2D Skeletonization Process on LV**



Source: prepared by G.Gökay with Matlab

**Figure 3.19: 2D Skeletonization Process on CS**



Source: prepared by G.Gökay with Matlab

For the 3D measurements we are going use volume, length, cross-sectional area, values based on LV and CS 3D segmentations to correlate results with experts' grades. To measure LV and CS length we use approach automatically. For the cross-sectional area values of the LV and CS we calculate the volume of the each LV or CS segmentation and then we divide volume to length to calculate average cross-sectional area. Results based on the calculations are given in the results part for both LV and CS.

## 4. RESULTS

Previous section summarized the computer based measurement methods we employed. This section presents the results obtained by using those methods and their detailed analyses.

### 4.1 MEASUREMENT AND CORRELATION RESULTS

2D and 3D measurements of both LV and CS structures are obtained automatically and their relationships with the expert atrophy ratings were examined using Pearson correlation analysis.

Tables 4.1, 4.2, 4.3 and 4.4 present these automatically obtained measurements for each subject in the database and the correlation scores between the measurements and the expert grades. The agreement between the measurements and the expert grades are further visualized via simple linear regression in Figures 4.1, 4.2, 4.3, and 4.4.

In this study, for correlation analysis the following scale is used: 0.00-to-0.29 no correlation, 0.30-to-0.49 weak correlation, 0.50-0.74 moderate correlation, 0.75-to-1.00 strong correlation.

#### 4.1.1 2D Measurement Results of LV

Exchanging ideas with experts in the project team and in the light of the literature review, the size of the lateral ventricles are expected to be associated with expert ratings. To this end, LV structure is automatically segmented using ALVIN and its area, width and length are automatically quantified from the segmentation at the axial slice corresponding to the largest LV area. These 2D measurements along with their correlations with expert grades and the related linear regression results are given in Table 4.1 and Figure 4.1, respectively.

In regard to the correlations of measurements with expert ratings, width and area of LV depict strong correlation values ( $\geq .80$ ) and confirms our prior expectation. This observation is further supported by the linear regression analysis visualized in Figure 4.1, where the goodness-of-fit ( $R^2$ ) scores for area and width are above 0.67 and are

more consistent between the two hemispheres while this score is observed to be lower and more varying for the length measure (0.39 for the left part and 0.61 for the right part).

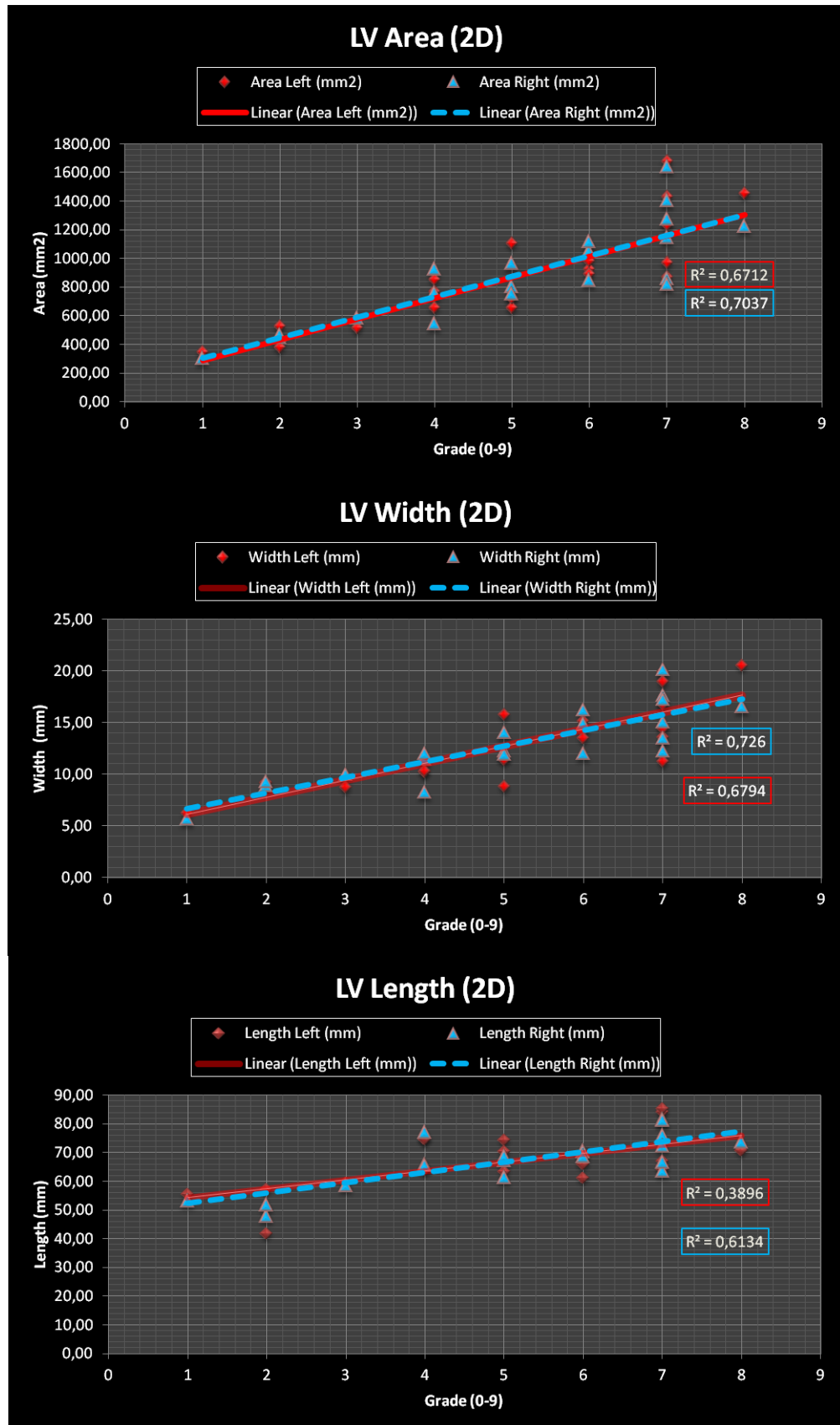
**Table 4.1: 2D LV Measurement Results**

Patient	Grade (0-9)	Area Left (mm <sup>2</sup> )	Area Right (mm <sup>2</sup> )	Width Left (mm)	Width Right (mm)	Length Left (mm)	Length Right (mm)
P1	8	1222,00	1452,76	16,56	20,51	73,80	70,84
P2	7	1639,90	1675,87	12,24	19,89	81,65	84,24
P3	7	1142,43	968,97	13,50	14,44	76,07	67,10
P4	7	1401,30	1429,45	17,59	16,73	81,45	85,44
P5	7	1275,48	1235,05	17,20	18,92	72,50	65,27
P6	7	859,39	871,78	15,02	13,55	63,64	64,35
P7	7	816,22	829,38	20,08	11,20	66,66	74,03
P8	6	1051,05	922,70	16,24	15,09	70,73	61,16
P9	6	846,61	979,04	12,00	14,21	70,57	68,92
P10	6	1118,73	892,11	14,86	13,50	68,89	66,07
P11	5	803,12	656,10	14,03	8,81	67,28	74,48
P12	5	752,73	722,03	12,23	11,36	61,54	63,53
P13	5	963,14	1107,37	11,94	15,74	68,64	70,36
P14	4	925,42	853,31	11,48	11,41	77,19	74,77
P15	4	544,90	654,92	8,26	10,22	66,01	64,07
P16	4	755,23	766,66	11,99	10,26	65,78	74,75
P17	3	582,39	518,00	9,95	8,73	58,56	59,34
P18	2	445,28	381,00	8,89	9,11	47,96	41,80
P19	2	462,32	528,14	9,28	9,22	52,03	57,31
P20	1	301,95	346,60	5,67	6,25	53,25	55,43
<b>Correlation</b>		<b>0,82</b>	<b>0,84</b>	<b>0,85</b>	<b>0,82</b>	<b>0,78</b>	<b>0,78</b>

Source: prepared by G.Gökay with Matlab



Figure 4.1: Scatter plots of 2D LV measurements versus expert grades



Source: prepared by G.Gökay with Excel

#### 4.1.2 2D Measurement Results of CS

Correlation between the 2D results for automatic measurements of CS (area, length and width) with expert ratings are presented in Table 4.2. CS measurement results are obtained from manual segmentations of CS and automatically calculated area, width and length values from the experiments that we have done.

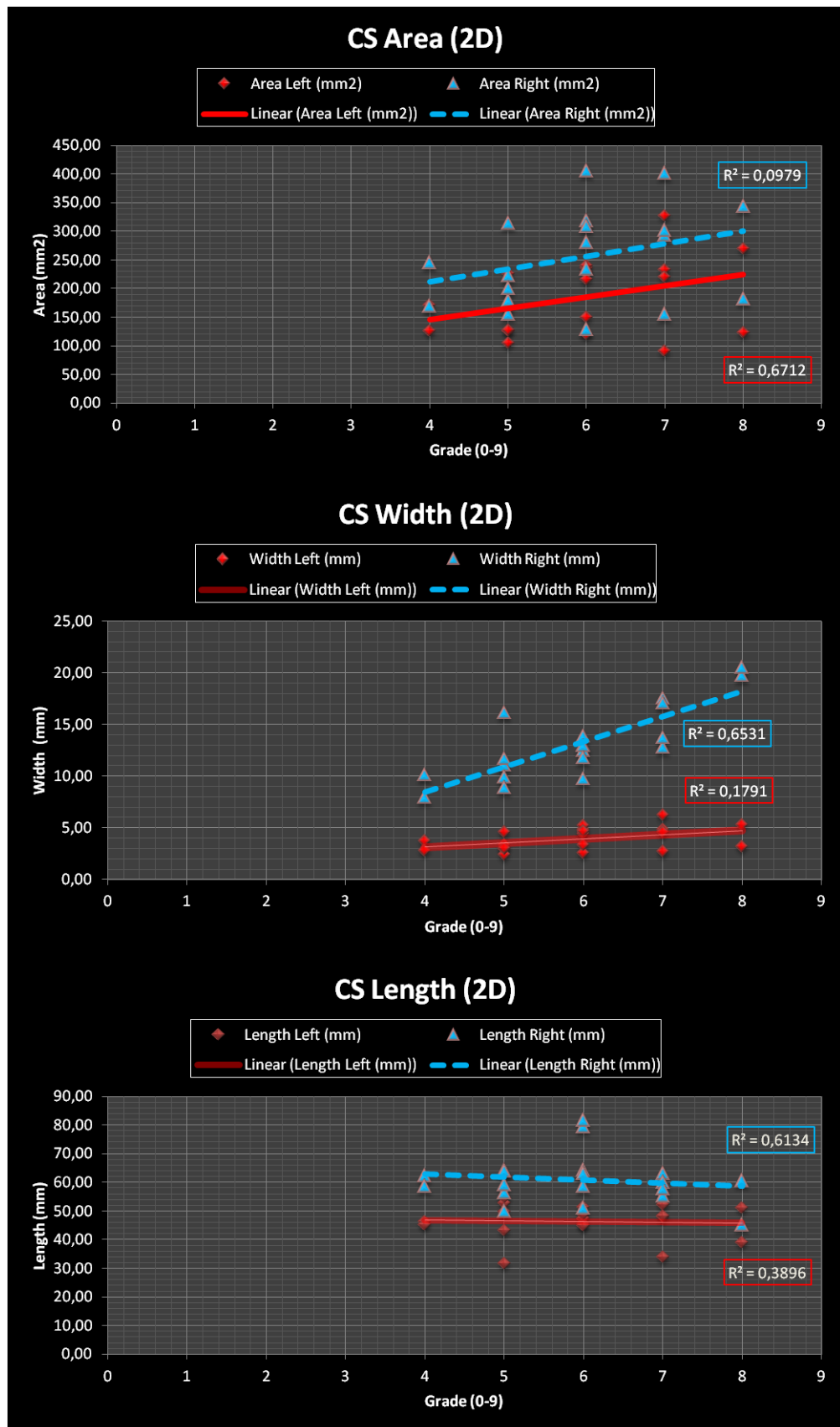
Correlation results in Table 4.2 show that, compared to the LV results, measurements of CS are less consistent with the degree of atrophy ( $\leq 50$ ). Similarly atrophy is associated with the width of CS width more than its length. Corresponding linear regression analysis visualized in Figure 4.2 also supports the above observations.

**Table 4.2: 2D CS Measurement Results**

Patient	Grade (0-9)	Area Left (mm <sup>2</sup> )	Area Right (mm <sup>2</sup> )	Width Left (mm)	Width Right (mm)	Length Left (mm)	Length Right (mm)
P1	8	269,03	343,17	5,26	5,65	51,13	60,74
P2	8	123,61	181,98	3,18	4,04	38,83	45,10
P3	7	326,22	401,91	6,24	6,37	52,31	63,14
P4	7	232,50	293,80	4,85	4,90	47,95	59,93
P5	7	90,80	154,88	2,68	2,80	33,83	55,22
P6	7	220,01	301,05	4,57	5,20	48,19	57,86
P7	6	227,96	280,72	4,85	5,49	47,04	51,15
P8	6	119,80	129,13	2,53	2,20	47,36	58,69
P9	6	235,24	405,86	5,19	6,30	45,35	64,39
P10	6	150,43	233,68	3,34	2,94	45,01	79,37
P11	6	216,06	319,05	4,44	3,91	48,69	81,62
P12	6	239,38	309,15	4,66	4,90	51,35	63,10
P13	5	225,99	314,70	4,56	5,59	49,54	56,33
P14	5	126,16	179,23	2,39	2,79	52,79	64,29
P15	5	127,46	223,54	2,96	3,77	43,07	59,34
P16	5	104,64	155,65	3,31	3,11	31,61	50,05
P17	5	164,31	200,99	3,00	3,14	54,75	64,02
P18	4	170,75	244,92	3,69	3,93	46,30	62,37
P19	4	125,75	169,49	2,78	2,89	45,19	58,56
<b>Correlation</b>		<b>0,36</b>	<b>0,31</b>	<b>0,42</b>	<b>0,39</b>	<b>-0,05</b>	<b>-0,15</b>

Source: prepared by G.Gökay with Matlab

Figure 4.2: Scatter plots of 2D CS measurements versus expert grades



Source: prepared by G.Gökay with Excel

### 4.1.3 3D Measurement Results of LV

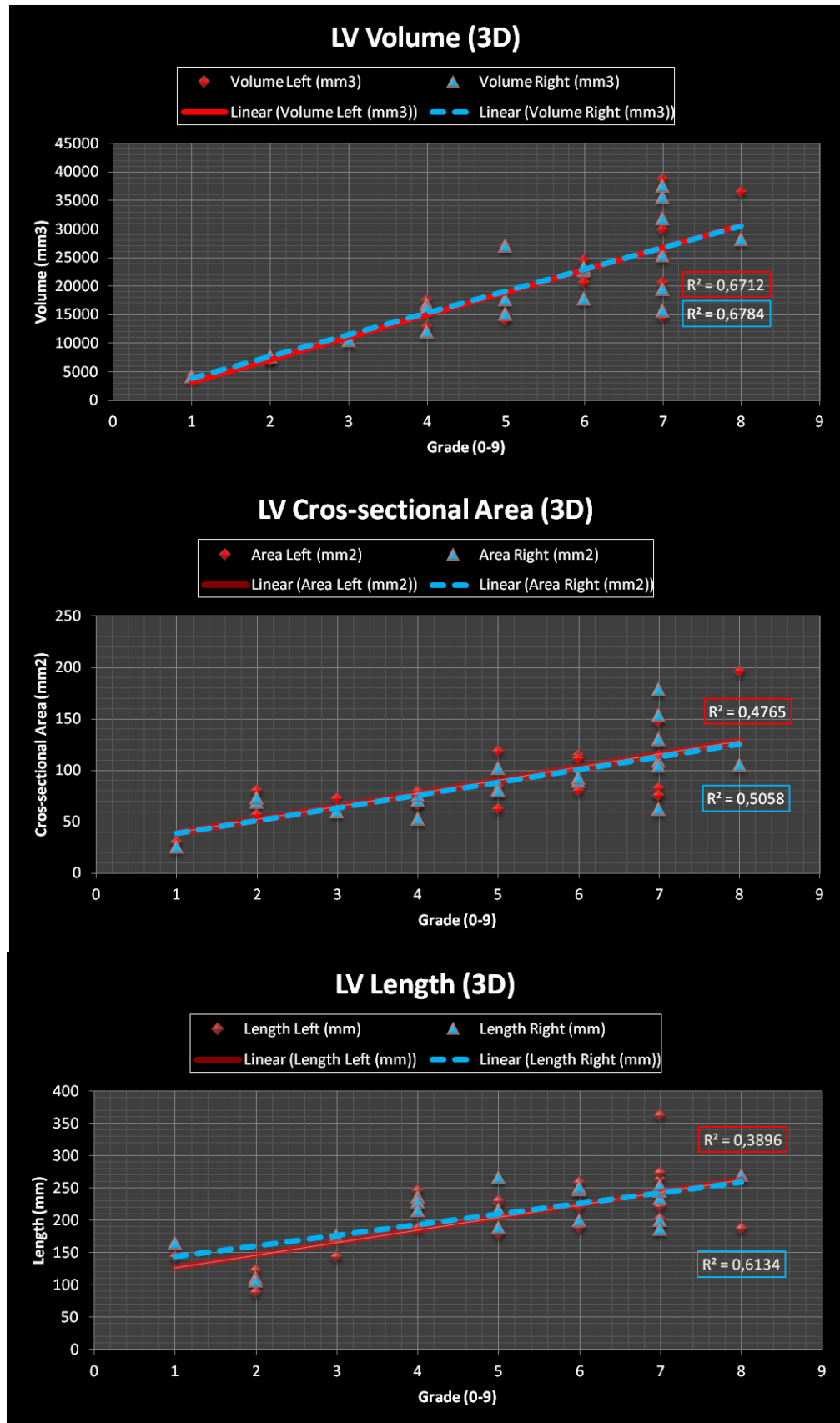
Automatic 3D measurements of LV (volume, cross-sectional area and length) and their correlations with expert ratings are presented in Table 4.3. As seen, LV volume shows strong correlation with grades ( $\geq 0.82$ ), while average cross-sectional area and length have moderate correlation values ( $\geq 0.69$  and  $\geq 0.65$ , respectively). Linear regression results presented in Figure 4.3 also support these observations.

**Table:4.3 3D LV Measurement Results**

Patient	Grade (0-9)	Volume Left (mm <sup>3</sup> )	Volume Right (mm <sup>3</sup> )	Area Left (mm <sup>2</sup> )	Area Right (mm <sup>2</sup> )	Length Left (mm)	Length Right (mm)
P1	8	36532,77	28242,32	195,78	105,03	186,60	268,89
P2	7	38695,91	35627,90	146,98	178,33	263,28	199,78
P3	7	25104,67	37559,29	113,89	153,25	220,43	245,09
P4	7	25774,69	25426,34	127,36	109,33	202,38	232,57
P5	7	29905,79	31854,93	82,76	130,07	361,36	244,90
P6	7	20566,04	19433,40	75,42	104,43	272,69	186,09
P7	7	14578,08	15648,93	75,34	61,88	193,49	252,90
P8	6	21495,74	22910,22	114,29	92,74	188,08	247,03
P9	6	24504,74	17815,94	111,68	89,52	219,41	199,03
P10	6	20562,19	23240,54	79,80	92,56	257,66	251,10
P11	5	14010,99	17648,42	61,96	82,01	226,12	215,21
P12	5	14999,20	15145,71	84,13	80,27	178,28	188,68
P13	5	27111,89	27133,24	118,41	102,10	228,96	265,76
P14	4	16335,92	16747,32	66,44	71,17	245,89	235,31
P15	4	12861,38	12054,12	68,65	52,70	187,36	228,75
P16	4	17506,94	16140,90	79,32	75,39	220,73	214,11
P17	3	10306,45	10531,65	72,24	59,82	142,67	176,06
P18	2	7132,22	7718,83	80,27	69,51	88,85	111,05
P19	2	6946,37	7683,98	56,77	73,04	122,36	105,21
P20	1	4259,04	4150,50	29,87	25,30	142,61	164,08
<b>Correlation</b>		<b>0,84</b>	<b>0,82</b>	<b>0,69</b>	<b>0,71</b>	<b>0,65</b>	<b>0,71</b>

Source: prepared by G.Gökay with Matlab

Figure 4.3: Scatter plots of 3D LV measurements versus expert grades



Source: prepared by G.Gökay with Excel

#### 4.1.4: 3D Measurement Results of CS

Table 4.4 presents automatic 3D measurements of CS (volume, cross-sectional area and length) and their correlation scores with expert ratings. In this analysis, expert manual segmentations of CS are used due to the very challenging nature of automatic CS segmentation in 3D. Nevertheless, quantification of the measurements (volume, cross-sectional area and length) from manual segmentations is achieved automatically.

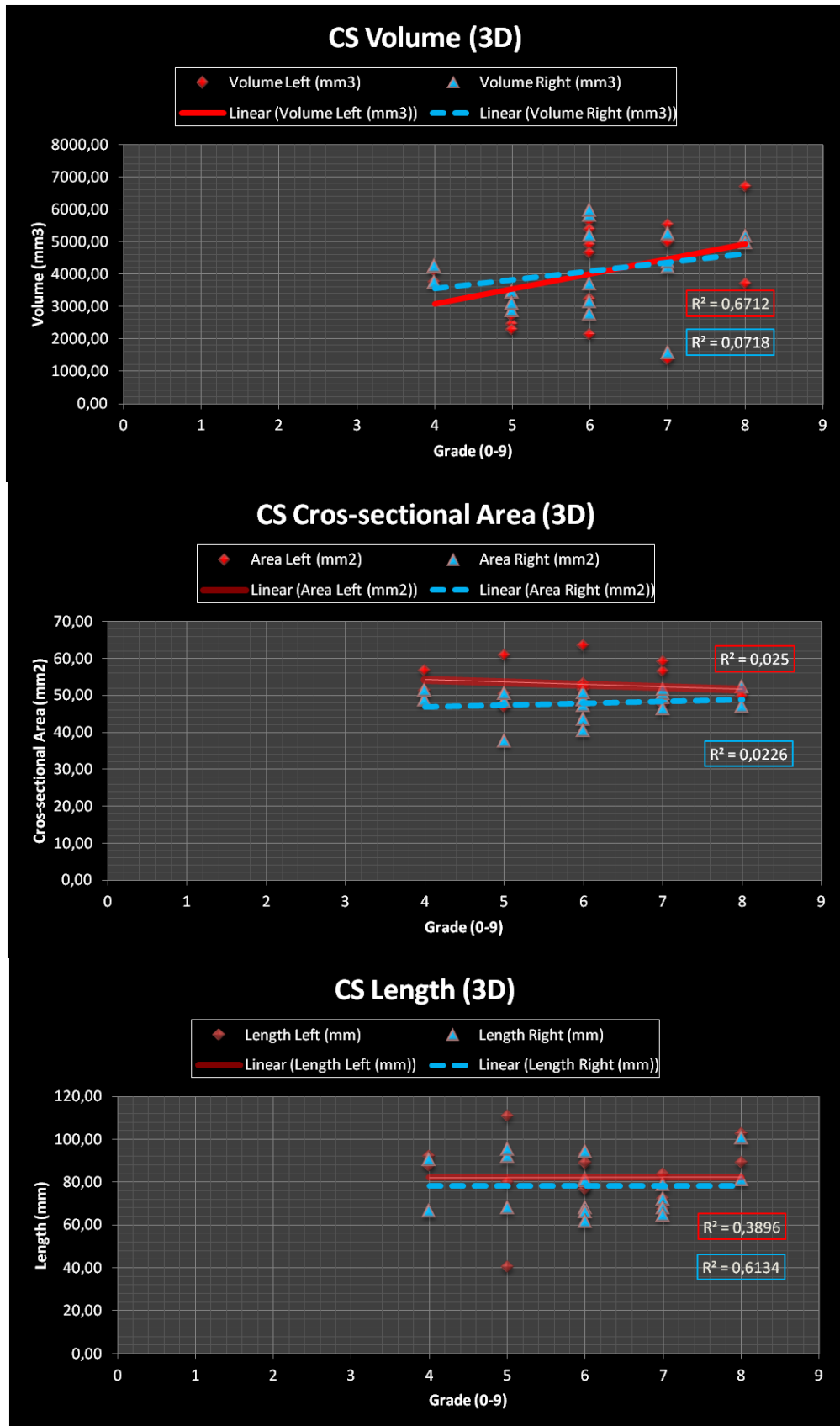
Results in Table 4.4 show that, as compared to the LV results, CS measurements have considerably lower correlation with the expert grades (degree of atrophy). This observation is also supported by the low and varying (between hemispheric measurements)  $R^2$  scores of regression analysis presented in Figure 4.4.

**Table 4.4: 3D CS Measurement Results**

Patient	Grade (0-9)	Volume Left (mm <sup>3</sup> )	Volume Right (mm <sup>3</sup> )	Area Left (mm <sup>2</sup> )	Area Right (mm <sup>2</sup> )	Length Left (mm)	Length Right (mm)
P1	8	6715,96	5195,06	50,87	47,20	88,94	100,71
P2	8	3704,99	4976,68	49,75	52,29	102,37	81,09
P3	7	5075,80	4241,38	56,53	49,47	69,01	72,05
P4	7	4995,27	4398,84	59,09	50,56	67,24	79,03
P5	7	1358,59	1584,54	47,54	46,42	72,30	68,16
P6	7	5530,54	5260,10	48,09	51,76	83,70	64,54
P7	6	4911,79	3707,66	63,46	43,67	76,55	67,89
P8	6	2151,04	2797,60	47,89	40,51	76,72	81,52
P9	6	5637,54	5204,39	52,86	47,45	93,14	66,15
P10	6	3241,20	3164,73	53,30	49,08	88,66	61,63
P11	6	4655,24	5842,69	51,58	48,94	78,50	94,18
P12	6	5378,00	5978,95	52,46	50,92	88,90	80,81
P13	5	2470,08	3466,07	60,96	37,70	40,52	91,94
P14	5	2290,90	2894,65	50,36	48,48	79,84	68,25
P15	5	2707,25	3115,47	46,96	50,55	110,94	95,35
P16	4	4101,07	3755,86	56,67	48,88	87,63	90,36
P17	4	3759,49	4272,86	51,35	51,60	92,13	66,51
<b>Correlation</b>		<b>0,37</b>	<b>0,27</b>	<b>-0,16</b>	<b>0,15</b>	<b>0,01</b>	<b>0,00</b>

Source: prepared by G.Gökay with Matlab

Figure 4.4: Scatter plots of 3D CS measurements versus expert grades



Source: prepared by G.Gökay with Excel

The measurement results that have relatively high correlations obtained from the works are given previously. For this time in the Table 4.5 show all work for the project including different manual segmentations from different experts to strengthen CS results which have lower correlation than LV results.

**Table 4.5: Correlation Results of the Database**

Data Information						Correlation Results (Pearson)					
#	Location	Dimension	Segmentation	Measurement	Number of Patients	Lenght		Width		Area	
						Right	Left	Right	Left	Right	Left
1	LV	2D	Manual	Manual	10	0,58	0,44	0,88	0,93	-	-
2	LV	2D	Automatic	Automatic	20	0,82	0,84	0,82	0,85	0,62	0,78
3	CS	2D	Manual	Manual	10	-0,30	-0,24	0,61	0,70	-	-
4	CS	2D	Manual(1)	Automatic	19	-0,15	-0,05	0,39	0,42	0,31	0,36
5	CS	2D	Manual(2)	Automatic	18	0,08	0,38	0,08	0,17	0,40	0,29
6	CS	2D	Automatic	Automatic	19	0,15	0,34	0,03	0,01	-0,03	0,17
#	Location	Dimension	Segmentation	Measurement	Number of Patients	Lenght		Cross Sectional Area		Volume	
						Right	Left	Right	Left	Right	Left
7	LV	3D	Automatic	Automatic	20	0,71	0,65	0,69	0,71	0,82	0,84
8	CS	3D	Manual(1)	Automatic	17	0	0,01	0,15	-0,16	0,27	0,37
9	CS	3D	Manual(2)	Automatic	19	-0,39	-0,07	-0,13	-0,10	0,34	0,34
10	CS	3D	Manual(1)	Semi-Automatic	20	0,17	-0,02	0,11	0,11	0,37	0,39

Source: prepared by G.Gökay with Matlab



## 5. DISCUSSION AND CONCLUSION

Various diseases occurring due to aging in the human brain have an important place in contemporary research as elderly population in the world and in our country are continuously increasing. As a result research focused on diagnosis and treatment of such diseases is needed. Computer-based measurement of cerebral atrophy, one of the biomarkers of dementia, and how it coincides with the severity of atrophy is not yet clear. Accordingly, in this thesis study computer-based measurement of cerebral atrophy from MR images is realized and compared to the experts' visual ratings.

Cerebral atrophy, defined as cell death dependent on tissue loss, affects part or all of the brain and is a feature observed in cases of dementia characterized as progressive impairment of memory and intellectual function beyond normal aging. To determine the presence and severity of cerebral atrophy, experts visually assess brain MR images for ventricular enlargement and/or sulcal widening.

Hence, the aim of this thesis was automatic size quantification of LV and CS from MR images, and comparison of these measurements' with atrophy ratings provided by field experts. In this study, we have developed image processing based approaches to compute the length, the width, the cross-sectional area, and the volume of LV and CS, and measured their agreement with atrophy ratings visually assessed by neurology and radiology experts for 20 subjects with memory complaints.

The patient set used in this study consists of subjects with varying levels of cerebral atrophy that are admitted to the hospital due to complaints of memory or cognitive ability. MR imaging of these subjects is done using a routine clinical protocol where image resolution (e.g. slice thickness) slightly varies. Automated quantification of cerebral atrophy from real brain MR data taken at routine clinical practice and comparing agreement between these quantifications and experts' visual assessments, as realized in this thesis work, is important because it provides a realistic insight regarding its predictive value.

The obtained results show that agreement with atrophy is more pronounced for lateral ventricle than central sulcus and for the width than the length of both structures in 2D

and 3D. Specifically, both automated and manual 2D measurements of lateral ventricle width show high agreement (around 0.85) with atrophy grades.

In addition, the 2D results obtained show higher correlations than those of 3D results. This might be due to the complexity of 3D measurements where errors at consecutive processing steps (e.g. segmentation and quantification) accumulate.

In general CS measurements have lower correlations as compared to those of LV, which might be attributed to segmentation errors of CS. Similar to the above observation, 2D measurements of CS show higher correlations than those obtained in 3D.

## **5.2 FUTURE WORKS**

This study opens up new questions that need further exploration. One such example is to evaluate the predictive power of the automated measurements in a larger cohort of healthy and demented cases. Another future work could be the cross-comparison of atrophy measurements obtained using the proposed approach and white matter hyperintensity load for different disease groups.

Also, redesigning 3D skeleton algorithm for the CS part to challenge with low correlation results could be a future work. Using partial differential equations to find skeleton might be the solution.

It is our sincere hope that the results and the methods presented in this thesis study will eventually pave the way for an accurate, robust, automated system that will aid the experts in dementia grading.

From this thesis, one paper has been published:

- i. Gökay, G., Kandemir, M., Tepe, M.S., Yalçın, B., Ünay, D., “Comparison of Cerebral Atrophy Grade with Sizes of Lateral Ventricle and Central Sulci, Sinyal İşleme ve İletişim Uygulamaları Kurultayı (SIU), Trabzon - Turkey, 2014.

We are planning to submit another publication summarizing the results of this work to an international journal in the near future.

## REFERENCES

### Books

Barkhof F, Fox NC, Bastos Leite AJ, Scheltens P. *Neuroimaging in Dementia*, 1st edn. New York: Springer, 2011.

Suetens P. 2009. *Fundamentals of Medical Imaging*, Cambridge University Press

Small J, Schaefer P. 2012. *Neuroradiology: Key Differential Diagnoses and Clinical Questions*, Saunders

Sethian, J.A. 1999. *Level Set Methods and Fast Marching Methods Evolving Interfaces in Computational Geometry, Fluid Mechanics, Computer Vision, and Materials Science*. Cambridge University Press.

## Periodicals

- Bell-McGinty S, Lopez OL, Meltzer CC, Scanlon JM, Whyte EM, Dekosky ST, Becker JT. 2005. Differential cortical atrophy in subgroups of mild cognitive impairment. *Arch Neurol.* **62**(9):1393-1397.
- Ekin A. Feature-based brain mid-sagittal plane detection by ransac, 2006. *Proc. EURASIP EUSIPCO*
- Ferri CP, Prince M, Brayne C, Brodaty H, Fratiglioni L, Ganguli M, Hall K, Hasegawa K, Hendrie H, Huang Y, Jorm A, Mathers C, Menezes PR, Rimmer E, Sczufca M; 2005. Alzheimer's Disease International. Global prevalence of dementia: a delphi consensus study. *Lancet*, **366**(9503):2112–2117.
- Giesel FL, Hahn HK, Thomann PA, Widjaja E, Wignall E, von Tengg-Kobligk H, Pantel J, Griffiths PD, Peitgen HO, Schroder J, Essig M. 2006. Temporal Horn Index and Volume of Medial Temporal Lobe Atrophy Using a New Semiautomated Method for Rapid and Precise Assessment, *AJNR Am J Neuroradiol.* **27**(7):1454-1458.
- Hassouna, M. S. et al. 2007. Multistencils Fast Marching Methods: A Highly Accurate Solution to the Eikonal Equation on Cartesian Domains, *IEEE transactions on pattern analysis and machine intelligence.* vol. 29, no:9.
- J. A. SETHIAN, 1996. A Fast Marching Level Set Method for Monotonically Advancing Fronts, *Proc. Nat. Acad. Sci.* vol. 93, nr. 4, pp. 1591-1595.
- Kempton, M.J. et al. 2011. A comprehensive testing protocol for MRI neuroanatomical segmentation techniques: Evaluation of a novel lateral ventricle segmentation method. *NeuroImage* **58**(4), 1051-1059
- MacKenzie JD, Siddiqi F, Babb JS, Bagley LJ, Mannon LJ, Sinson GP, Grossman RI. 2002. Brain atrophy in mild or moderate traumatic brain injury: a longitudinal quantitative analysis, *AJNR Am J Neuroradiol.* **23**(9):1509-15.

- Miller BL. 2002. Past Glory and Future Promise: Maximizing and Improving Understanding of Atrophy Patterns in the Diagnosis of Degenerative Dementias. *AJNR Am J Neuroradiol.* **23**(1):33–34
- Naidich TP, Brightbill TC. 1996. Systems for localizing frontoparietal gyri and sulci on axial CT and MRI. *Int J Neuroradiol* 2:313-388.
- Nestor, S.M. et al. 2008. Ventricular enlargement as a possible measure of alzheimer's disease progression validated using the alzheimer's disease neuroimaging initiative database. *Brain*, **131**(9), 2443–2454
- Portaccio et al. 2012. Natalizumab may reduce cognitive changes and brain atrophy rate in relapsing-remitting multiple sclerosis: a prospective, non-randomized pilot study. *Eur J Neurol.*
- Robert Van Uitert and Ingmar Bitter. 2007 Subvoxel precise skeletons of volumetric data based on fast marching methods. *Med. Phys.* 34, 627.
- Raya SP. 1990. Low-level segmentation of 3-D magnetic resonance brain images-a rule-based system. *IEEE Trans Med Imaging.* **9**(3):327-37.
- Rettmann ME, Kraut MA, Prince JL, Resnick SM. 2006. Cross-sectional and longitudinal analyses of anatomical sulcal changes associated with aging. *Cereb Cortex.* **16**(11):1584-1594.
- Scheltens P, Leys D, Barkhof F, Huglo D, Weinstein HC, Vermersch P, Kuiper M, Steinling M, Wolters EC, Valk J. 1992. Atrophy of medial temporal lobes on MRI in "probable" Alzheimer's disease and normal ageing: diagnostic value and neuropsychological correlates. *J Neurol Neurosurg Psychiatry.* **55**(10):967-972.
- Scher AI, Xu Y, Korf ES, White LR, Scheltens P, Toga AW, Thompson PM, Hartley SW, Witter MP, Valentino DJ, Launer LJ. 2007. Hippocampal shape analysis in Alzheimer's disease: a population-based study. *Neuroimage.* **36**(1):8-18.
- Silverman DH, Small GW, Phelps ME. 1999. Clinical value of neuroimaging in the diagnosis of dementia: Sensitivity and specificity of regional cerebral metabolic

- and other parameters for early identification of alzheimer's disease. *Clinical Positron Imaging*, **2**(3):119–130.
- Soille, P., 2003. Morphological Image Analysis: Principles and Applications, 2nd Edition, Secaucus, NJ, Springer-Verlag, pp. 219–221.
- Tosun D, Duchesne S, Rolland Y, Toga AW, Verin M, Barillot C. 2007. 3-D analysis of cortical morphometry in differential diagnosis of Parkinson's plus syndromes: mapping frontal lobe cortical atrophy in progressive supranuclear palsy patients. *Med Image Comput Comput Assist Interv*. 10(Pt 2):891-9,
- van de Pol LA, Verhey F, Frisoni GB, Tsolaki M, Papapostolou P, Nobili F, Wahlund LO, Minthon L, Frolich L, Hampel H, Soininen H, Knol DL, Barkhof F, Scheltens P, Visser PJ. 2009. White matter hyperintensities and medial temporal lobe atrophy in clinical subtypes of mild cognitive impairment: the DESCRIPA study. *J Neurol Neurosurg Psychiatry*. **80**(10):1069-1074.
- Whitwell JL, Petersen RC, Negash S, Weigand SD, Kantarci K, Ivnik RJ, Knopman DS, Boeve BF, Smith GE, Jack CR Jr. 2007. Patterns of atrophy differ among specific subtypes of mild cognitive impairment. *Arch Neurol*. **64**(8):1130-1138
- Waldemar G, Dubois B, Emre M, Scheltens P, Tariska P, Rossor M. 2000. Diagnosis and management of alzheimer's disease and other disorders associated with dementia. The role of neurologists in Europe. *European Journal of Neurology*, **7**(2):133–144,
- Yue, N.C. et al. 1997. Sulcal, ventricular, and white matter changes at mr imaging in the aging brain: data from the cardiovascular health study. *Radiology*, **202**(1), 33–39

## **Others**

Cankurtaran M., Ariođul S. 2004. Alzheimer hastalıđı ve vasküler demansta risk faktörleri. *Hacettepe Üniversitesi İç Hastalıkları AD Geriatri Ünitesi Yan dal uzmanlık tezi,*

Demir O. 2013. Automatic segmentation of central sulcus on brain MR images. *MSc Thesis, Bahçeşehir University*

Haralick and Shapiro 1992. Computer and Robot Vision, *Addison-Wesley* pp.170-171

Hayashi, N., 2010. Development of identification of the central sulcus in brain. *Radiol Phys Technol.*

## CURRICULUM VITAE

**Name Surname:** Gökhan GÖKAY

**Address:** Üsküdar/ İstanbul

**Date and Place of Birth:** Antalya – 11.02.1989

**Foreign Language:** English, Russian

**Elementary Education:** Antalya Namık Kemal İlköğretim Okulu, 2003

**Secondary Education:** Antalya HMM Bileydi Anadolu Lisesi, 2007

**Undergraduate Education:** Bahcesehir University, Electrical & Electronics Eng., 2012

**Graduate Education:** Bahcesehir University, Bioengineering, Present

**Name of Institute:** Graduate School Of Natural And Applied Sciences

**Name of Program:** BioEngineering

**Work Experience:**

- Bahcesehir University – Research Asistant – 2012–2014
- Figes AŞ – Matlab Application Engineer – 2014 – Present